© 2018. Published by The Company of Biologists Ltd | Journal of Experimental Biology (2018) 221, jeb189647. doi:10.1242/jeb.189647

RESEARCH ARTICLE

Insect fat body cell morphology and response to cold stress is modulated by acclimation

Lauren E. Des Marteaux[1,*], Tomáš Štětina[1,2] and Vladimír Koštál[1]

ABSTRACT

Mechanistic understanding about the nature of cellular cryoinjury and mechanisms by which some animals survive freezing while others do not is currently lacking. Here, we exploited the broadly manipulable freeze tolerance of larval malt flies (*Chymomyza costata*) to uncover cell and tissue morphological changes associated with freeze mortality. Diapause induction, cold acclimation and dietary proline supplementation generate malt fly variants ranging from weakly to extremely freeze tolerant. Using confocal microscopy and immunostaining of the fat body, Malpighian tubules and anterior midgut, we described tissue and cytoskeletal (F-actin and α-tubulin) morphologies among these variants after exposure to various cold stresses (from chilling at −5°C to extreme freezing at −196°C), and upon recovery from cold exposure. Fat body tissue appeared to be the most susceptible to cryoinjury: freezing caused coalescence of lipid droplets, loss of α-tubulin structure and apparent aggregation of F-actin. A combination of diapause and cold acclimation substantially lowered the temperature at which these morphological disruptions occurred. Larvae that recovered from a freezing challenge repaired F-actin aggregation but not lipid droplet coalescence or α-tubulin structure. Our observations indicate that lipid coalescence and damage to α-tubulin are non-lethal forms of freeze injury, and suggest that repair or removal (rather than protection) of actin proteins is a potential mechanism of acquired freeze tolerance.

KEY WORDS: Freeze tolerance, *Chymomyza*, Diapause, Cytoskeleton, Actin, Drosophilid

INTRODUCTION

Insects employ a variety of strategies to survive at low temperatures, and while the majority of those studied (an estimated 70%) are freeze intolerant (Sinclair et al., 2003), the most cold-hardy species survive internal freezing (Worland et al., 2004; Sformo et al., 2010; Li, 2016). Currently, we lack mechanistic understanding about how the cells of some insects survive freezing, and whether survival links to protection or repair of cryoinjury (Pegg, 2007; Clark and Worland, 2008; Gosden, 2011; Štětina et al., 2018; Toxopeus and Sinclair, 2018). Uncovering these basic principles of insect overwintering physiology is imperative for predicting species' distributions and responses to climate change, and also has great potential for applied research; e.g. the efficacy of cold storage of insects (e.g. for biological control) is often limited by the detrimental effects of low temperatures on development, fecundity, performance and survival (Bloem et al., 2006; Colinet and Boivin, 2011). Manipulation of freeze tolerance is therefore crucial for production and management of quality arthropod stock populations and is the ultimate goal in cryopreservation of biological material (Leopold, 1991, 2007; Ayvaz et al., 2008; Ghazy et al., 2012).

Insect cold tolerance is considerably plastic (Ayrinhac et al., 2004; Kvist et al., 2013; Sgrò et al., 2016), and cold acclimation or dietary manipulation can even induce freeze tolerance in otherwise freeze-intolerant insects (Koštál et al., 2011a, 2012; McKinnon, 2015). The malt fly, *Chymomyza costata* (Zetterstedt 1838) (Diptera: Drosophilidae), is an emerging model for understanding freeze tolerance mechanisms and plasticity in insects (Koštál et al., 2003, 2011a, 2016; Rozsypal et al., 2018; Štětina et al., 2018). Cold tolerance in this species is broadly manipulable; active larvae tolerate freezing only at mild subzero temperatures (e.g. −5°C), but under appropriate rearing conditions the larvae can survive exposure to −196°C, making malt flies one of only a few animals known to withstand such extreme freezing in a hydrated state (Van Wyk et al., 1977; Ramløv and Westh, 1992; Moon et al., 1996; Suzuki et al., 2014). Survival of malt flies at −196°C is achieved by the combined effects of diapause and cold acclimation, but even dietary proline supplementation alone confers extreme freeze tolerance for some individuals (Koštál et al., 2011b). The mechanisms by which acclimation and dietary manipulation confer freeze tolerance are not well resolved.

Freezing presents multiple physiological challenges for the cell: rapid ice crystal formation can damage the cells mechanically, while growth of extracellular ice results in cellular dehydration stress linked to increased acidity, viscosity, toxic metabolic intermediate concentrations, macromolecular crowding and hyperosmotic shock (Neufeld and Leader, 1998; Minton, 2000; Storey and Storey, 2012; Pegg, 2015). These changes in the intracellular environment should severely threaten the chemical and conformational stability of proteins and other macromolecules (Hazel, 1995; Hochachka and Somero, 2002; Bhatnagar et al., 2007; Dias et al., 2010). As direct observation of such molecular damage is technically difficult, the effects of freezing are most often observed at the whole-organism level (via survival analysis). To bridge the gap between loss of molecular function and whole-organism survival, we can first look for evidence of cryoinjury at two technically feasible levels: cells and tissues. The insect midgut and fat body tissues appear to be particularly susceptible to freezing damage (Izumi et al., 2005; Teets et al., 2011). Freezing also damages the Malpighian tubules of freeze-tolerant insects (Neufeld and Leader, 1998; Marshall and Sinclair, 2011). Cytoskeletal proteins (e.g. actin and tubulin) are readily observable structural components of the cell that are modified by both cold stress (Belous, 1992; Russotti et al., 1997; Cottam et al., 2006; Kayukawa and Ishikawa, 2009) and cold acclimation (Michaud and Denlinger, 2004; Kim et al.,

[1]Institute of Entomology, Biology Centre of the Academy of Sciences of the Czech Republic, 370 05 České Budějovice, Czech Republic. [2]Faculty of Science, University of South Bohemia, Branišovská 31, 370 05 České Budějovice, Czech Republic.

*Author for correspondence (ldesmart@uwo.ca)

L.E.D., 0000-0002-0461-2704; V.K., 0000-0002-4994-5123

Received 1 August 2018; Accepted 3 September 2018

Journal of Experimental Biology (2018) 221, jeb189647. doi:10.1242/jeb.189647

List of abbreviations

LD	long-day, non-acclimated larvae (active, freeze intolerant)
LD	long-day, non-acclimated larvae supplemented with 50 mg proline per 1 g diet (active, moderately freeze tolerant)
NGS	normal goat serum
PB	phosphate buffer
PBT	phosphate buffer with 0.5% Triton X-100
SC	supercooled larvae (remaining unfrozen)
SDA	short-day, cold-acclimated larvae (diapause, extremely freeze tolerant)

2006; Teets et al., 2012; Gerken et al., 2015; Des Marteaux et al., 2018), making them ideal indicators of freeze-attributed cellular damage.

We aimed to identify freeze-attributed changes to cell and tissue morphology that are associated with insect mortality. Using microscopy and immunostaining, we characterized the effects of lethal and sublethal cold stress on morphology of the fat body, Malpighian tubules and anterior midgut in malt fly larvae. Specifically, we compared cell morphology and cytoskeletal structure (F-actin and α-tubulin) of weakly freeze-tolerant (non-diapause) and extremely freeze-tolerant (acclimated, diapausing) malt fly larvae exposed to various cold stresses (from chilling at −5°C to extreme freezing at −196°C) and upon recovery from cold exposure. We also characterized the effects of dietary proline supplementation (which confers freeze tolerance to non-acclimated malt flies; Koštál et al., 2011a; Rozsypal et al., 2018) on cell morphology after freezing. We predicted that cell structure would be resistant to disruption by a freezing challenge and/or repaired during recovery in freeze-tolerant malt flies, but would be disrupted by a freezing challenge in freeze-intolerant malt flies, and that this protection or repair would correlate with survival.

MATERIALS AND METHODS

Malt fly rearing, acclimation and cold exposure

A malt fly (*Chymomyza costata*) strain (Sapporo) originating from Sapporo, Hokkaido, Japan (Riihimaa and Kimura, 1988), was reared on an artificial diet (52 g malted barley, 28 g corn meal, 18 g dry yeast, 10 g agar powder, 1.7 g methyl hydroxybenzoate per 1.0 liter water) in mass colonies. Adults were housed in 200 ml glass jars containing 10 ml of diet. To collect eggs, a few drops of live yeast suspension were added to fresh apple pieces and kept overnight, after which they were added to flasks containing adults. Females oviposited on the apple for 3 days before the apple pieces were moved to 3×10 cm cylindrical glass vials containing 10 ml of diet and one drop of live yeast suspension. These vials contained developing larval populations of up to 200 individuals. Adult and larval colonies were housed in a Lovibond® ET 650-8 incubator (Tintometer GmbH, Dortmund, Germany) at 18°C and a 16 h:8 h light:dark photoperiod.

Malt flies were reared from eggs to third instar larvae under different temperature and photoperiod or diet regimes to produce larvae of three different cold tolerance states: (1) weakly freeze tolerant ‘long-day’ (LD); (2) moderately freeze tolerant ‘long-day, proline-supplemented’ (LD Pro50); and (3) extremely freeze tolerant ‘short-day acclimated’ (SDA). LD and LD Pro50 malt flies were reared under warm, long-day (colony) conditions at 18°C and a 16 h:8 h light:dark photoperiod, and the latter group was supplemented with 50 mg proline per gram diet. SDA larvae were first reared for 6 weeks in a Lovibond® ET 650-8 incubator at 18°C and a shorter day length (12 h:12 h light:dark, which initiates diapause; Koštál et al., 2016), transferred to an MIR 154 incubator (Sanyo Electric, Osaka, Japan) at 11°C and constant darkness for 1 week, and finally placed in a refrigerator at 4°C and constant darkness for 4 weeks (rearing and acclimation details in Fig. S1). Just over 70% of LD larvae survive to adulthood after supercooling at −5°C, while only 39% reach adulthood after freezing at −5°C (and none survive after exposure to −20°C) (Rozsypal et al., 2018). Almost half of LD Pro50 larvae reach adulthood even after freezing to as low as −40°C (Koštál et al., 2011a). For SDA larvae, just over 75% survive to adulthood after freezing to temperatures as low as −75°C, and approximately half reach adulthood after long-term exposure (6 months) to −196°C in liquid nitrogen (LN_2). SDA larval survival and successful emergence after LN_2 exposure requires pre-freezing to −30°C; this temperature marks the completion of glass transition for body liquids (which does not occur at pre-freezing to −20°C). Survival among treatments is listed in Table 1, from Rozsypal et al. (2018).

For cold exposure treatments, larvae were placed between two pieces of moistened cellulose in plastic tubes and immersed in a programmable Ministat 240 bath (Huber, Offenburg, Germany). Temperature inside the tubes was monitored using type T thermocouples and PicoLog software (Pico Technology, Cambridge, UK). Tubes were gradually cooled at 0.1°C min^{-1} from 0 to −5°C (with and without freezing), −20°C and −30°C, held at the target temperature for 1 h, and then warmed at 0.6°C min^{-1} to 5°C. Some larvae cooled to −20 or −30°C were immediately plunged into LN_2 for 1 h and then returned to −20 or −30°C, from which they were warmed. Fewer than 20% of SDA larvae survive LN_2 exposure if first cooled to −20°C, while nearly all survive LN_2 if first cooled to −30°C (this temperature likely allows larvae to complete the glass transition of body liquids) (Rozsypal et al., 2018). To separate the effects of temperature and freezing on cell morphology, larvae at −5°C were either supercooled (i.e. remained unfrozen; ‘−5°C SC’ treatment) or frozen by adding an ice crystal to the tube to promote inoculation (‘−5°C F’ treatment). Supercooling or freezing of the larvae was verified by the absence or presence of an exotherm (indicating heat released upon freezing), respectively. All cold exposure details are provided in Fig. S2A. To determine whether disruptions to cell morphology are repaired or persist upon recovery from sublethal freezing, some larvae were returned to colony rearing conditions and dissected after 3 days (LD −5°C F), 1 week (SDA −30°C) or at the prewandering stage (approximately 3 weeks; SDA −30°C).

Immunohistochemical staining and imaging

We dissected larvae in chilled PBS (137 mmol l^{-1} NaCl, 2.7 mmol l^{-1} KCl, 10 mmol l^{-1} $Na_2HPO_4{\cdot}2H_2O$, 1.8 mmol l^{-1} KH_2PO_4, pH 7.2) under a dissecting microscope either directly from rearing conditions (LD and LD Pro50 at 18°C, SDA at 4°C) or immediately after cold exposure regimes. Internal organs (the entire alimentary canal including the Malpighian tubules, and fat body) were extracted from each larva in a single mass and fixed overnight (17–18 h) at room temperature with 4% paraformaldehyde in PB (0.8 mol l^{-1} $Na_2HPO_4{\cdot}7H_2O$, 0.2 mol l^{-1} $NaH_2PO_4{\cdot}2H_2O$, pH 7.4). Tissue masses were rinsed 3×15 min in PB, permeabilized for 20 min in PBT (PB with 0.5% Triton X-100), blocked for 4 h in PBT with 5% normal goat serum (NGS), and immersed in 5% NGS containing a 1:12 dilution of α-tubulin primary antibody (anti-α-tubulin 12G10, Developmental Studies Hybridoma Bank, University of Iowa, USA) at 4°C overnight (17–18 h). After 3×15 min washing in PBT, tissues were then hybridized in 5% NGS containing a 1:200 dilution of secondary

Journal of Experimental Biology (2018) 221, jeb189647. doi:10.1242/jeb.189647

antibody (goat anti-mouse Alexa Fluor® 647; Abcam, Cambridge, UK) for 24 h at 4°C. After 3×15 min rinsing in PBT, tissues were stained with a 1:100 dilution of Alexa Fluor® 488 phalloidin (Life Technologies, Carlsbad, CA, USA) in PBT for 20 min and rinsed again for 3×15 min. The fat body, entire gut and Malpighian tubules were arranged on glass slides in ProLong™ Diamond antifade mountant with DAPI (Life Technologies) under a cover slip and sealed with clear nail polish. Slides were kept in the dark at 4°C until imaging.

We imaged the Malpighian tubules, anterior midgut and fat body (mid-section and surface) with a Confocal Olympus FluoView FV1000 microscope system (Olympus Europa) at 40× magnification in brightfield and excitation/emission wavelengths of 405/461 nm for DAPI (nuclei), 488/520 nm for phalloidin (F-actin) and 635/668 nm for α-tubulin antibody. We compared cell morphology among 15 treatments in total (Table S1). The number of larvae (biological replication) for each treatment was as follows: anterior midgut, n=9–12; Malpighian tubules, n=10–14; fat body mid-section, n=10–20; and fat body surface, n=9–20. We collected approximately two to four images (technical replicates) per biological replicate for each tissue. For details on biological and technical replication, see Figs S5–S10. Because we discovered that some freezing treatments cause F-actin aggregation (spotting) on the fat body surface, we compared the proportions of cells with many and/or large spots among LD treatments (excluding Pro50) and among SDA treatments (excluding LN_2) using ANOVA on arcsine-transformed data and determined pairwise differences using Tukey's honestly significant difference (HSD) tests. Differences in spotting between LD Pro50 treatments and between SDA LN_2 treatments were determined using Welch's t-tests. All statistical analyses were performed in R (v3.4.4; https://www.r-project.org/) with α=0.05.

RESULTS

To characterize cell morphologies among different malt fly freeze tolerance variants and cold exposures (15 treatments), we analyzed a total of 2706 tissue images: 1052 fat body mid-sections (526 each for brightfield and combined fluorescence stains), 920 fat body surfaces (460 each for F-actin and α-tubulin), 432 Malpighian tubules and 302 anterior midguts (151 each of epithelia and muscle by α-tubulin and F-actin staining, respectively). We also assessed the extent of F-actin aggregation (spotting) for 6400 fat body cells.

Freezing caused a coalescence of malt fly fat body lipid droplets (represented by SDA larvae in Fig. 1, all treatments in Figs S4 and S5), and our preliminary work indicates that coalescence relates primarily to temperature rather than to time frozen (although time has some effect on LD larvae; Figs S2 and S3). Lipid coalescence was indeed modulated by temperature but also by freeze-tolerance status; coalescence did not occur at −5°C (with or without freezing), was substantial for LD larvae frozen at −20°C (a lethal temperature; Fig. 2), but was only apparent in SDA larvae if frozen to −30°C (a sublethal temperature). Coalescence became entire (formation of a single large lipid droplet displacing nucleus and cytoplasm to the periphery) upon recovery and persisted at least until the prewandering stage.

Freezing of the fat body was accompanied by disintegration of α-tubulin radial structure and (often) a displacement of the nucleus (represented by LD larvae in Fig. 2, all treatments represented in Fig. S5). This loss of tubulin radial structure was most prominent in lethally frozen LD larvae, whose fat bodies were irregular even compared with those of lethally frozen SDA larvae. In addition, the fine mesh structure of α-tubulin on the periphery of fat cells appeared to differ among control, lethally frozen and recovered larvae (described in more detail in Fig. S6); however, these differences were subtle. α-Tubulin disruption in the fat cell interior was not repaired by

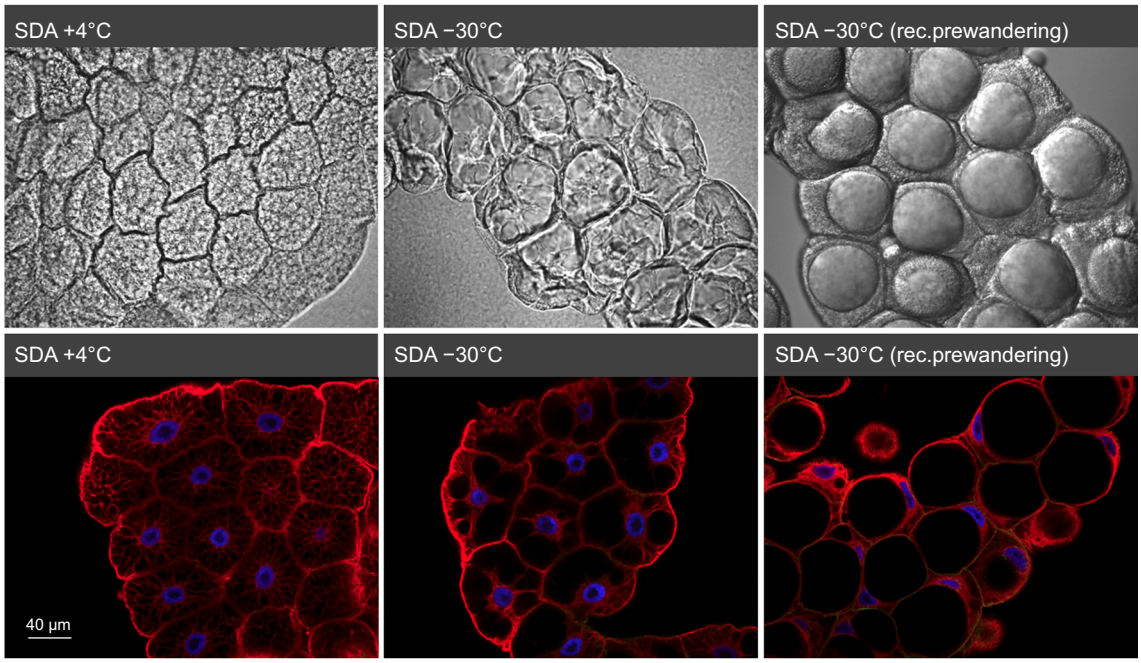

Fig. 1. Lipid droplet morphology in fat body cells before sublethal freezing (left), upon sublethal freezing (middle) and after recovery to the prewandering stage (right) in cold-acclimated, diapausing (SDA) malt fly larvae (confocal microscopy, mid-section). Top panels: brightfield; bottom panels: fluorescence staining for α-tubulin (anti-α-tubulin antibody, red), F-actin (phalloidin, green, generally not visible) and nuclei (DAPI, blue). n=10 larvae per treatment (~3 technical replicate images per larva). Freezing to −30°C caused substantial coalescence of lipid droplets, but this coalescence became complete (single large lipid droplet) during recovery and persisted at least until the prewandering stage. The influence of exposure temperature on droplet coalescence in LD and SDA larvae is corroborated in detail in Fig. S2. For representative images of all 15 treatments, see Figs S4 (brightfield) and S5 (fluorescence).

Journal of Experimental Biology (2018) 221, jeb189647. doi:10.1242/jeb.189647

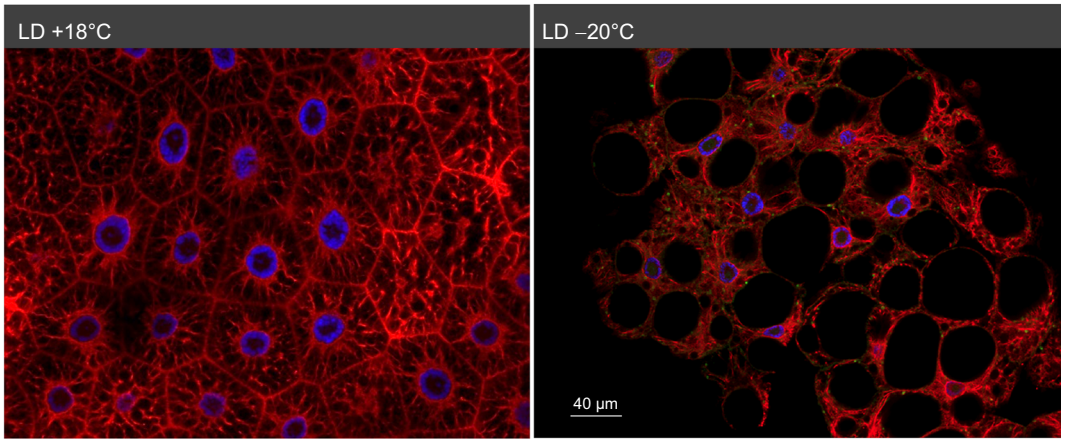

Fig. 2. Morphology of α-tubulin in the fat body of unfrozen (left) and lethally frozen (right) active, long-day-reared (LD) malt fly larvae (confocal microscopy, mid-section). Fluorescence staining: α-tubulin (anti-α-tubulin antibody, red), F-actin (phalloidin, green) and nuclei (DAPI, blue). *n*=14 to 20 larvae per treatment (~3 technical replicate images per larva). Freezing caused a loss of tubulin radial structure, coalescence of lipid droplets, and displacement of the nucleus. For representative images of fat body mid sections in all 15 treatments, see Fig. S5.

larvae that survived a freezing challenge (SDA larvae, Fig. 1). The fat body cells of LD larvae exposed to lethal freezing at –20°C exhibited some surface wrinkling (Fig. S7), but all SDA larvae exhibited substantial wrinkling of the fat body cell surfaces prior to freezing and even following recovery (Fig. 3; Figs S6 and S7).

Freezing was associated with the formation of apparent F-actin aggregates (spots) at the periphery of fat body cells (Fig. 4; Fig. S7). The extent of this aggregation differed by freeze tolerance status, and aggregates disappeared upon recovery (LD: $F_{4,64}$=26.4, P<0.001; SDA: $F_{5,54}$=30.2, P<0.001). In LD larvae, F-actin aggregates appeared in fat body cells when frozen at −5°C but were rare or absent if cells were merely supercooled to −5°C. Fat bodies of LD larvae lethally frozen to −20°C also exhibited F-actin aggregation; however, this was more variable among individuals. Cold acclimation lowered the temperature at which aggregates appeared: we observed aggregates in the SDA larval fat body only upon freezing to −30°C (none were apparent at −5 or −20°C).

Cell and tissue morphologies of SDA larvae exposed to LN_2 after pre-freezing to −20 and −30°C were very similar (Figs S4–S10). Fat body lipid droplet coalescence and loss of α-tubulin radial structure in both variants was severe, and both exhibited fat body F-actin aggregation. Proline supplementation produced variable morphological responses to freezing in malt fly larval tissues. For example, the extent of lipid droplet coalescence in LD Pro50 larvae exposed to −20°C ranged from none to severe (Fig. S5). Frozen LD Pro50 larvae also exhibited the highest proportion (87%) of fat body cells with F-actin aggregate spots (Fig. S7), and all Malpighian tubules exhibited lumenal F-actin spotting (Fig. 5). Supplementation with proline caused surface wrinkling in some fat body cells at 18°C (albeit to a lesser degree than in SDA larvae; Figs S4 and S7).

Anterior midgut and Malpighian tubule morphologies were generally unchanged among freeze tolerance variants and cold exposures (represented by various treatments in Fig. 6, all treatments in Figs S8–S10), with the exception of F-actin in the Malpighian tubule lumen (above). Sublethal freezing to −5°C (LD) and −30°C (SDA) caused lumen F-actin aggregation in approximately 14 and 50% of the Malpighian tubules, respectively, which disappeared completely upon recovery ($F_{9,94}$=8.46, P<0.001). F-actin aggregates were not apparent in the LD −20°C variant.

DISCUSSION

We expected to observe major morphological differences between unfrozen and frozen malt fly tissues and among different larval freeze tolerance variants; however, only the fat body generally exhibited obvious differences at the level of resolution investigated here. Furthermore, some of the apparent freezing injuries in fat body tissue were unrelated to mortality; it is unclear how these structural

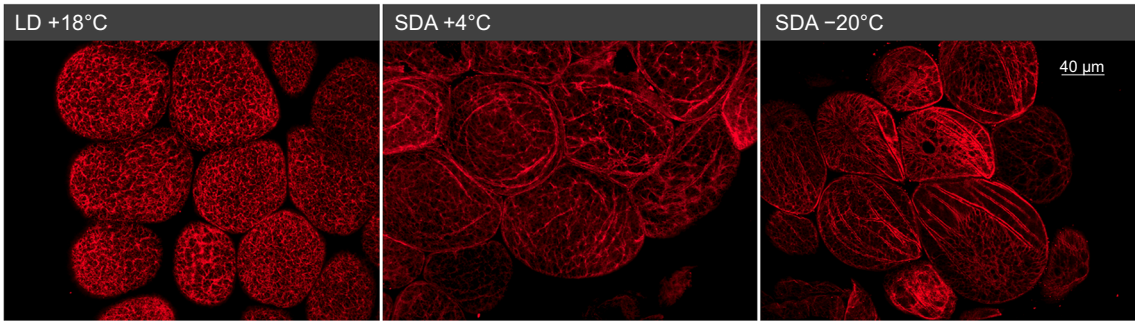

Fig. 3. Morphology of the fat body cell periphery in freeze-intolerant (LD) and freeze-tolerant (SDA) malt fly larvae, as shown by α-tubulin staining (anti-α-tubulin antibody, confocal microscopy). *n*=10 to 20 larvae per treatment (~3 technical replicate images per larva). Unlike in LD larvae, SDA larvae exhibit fat body cell surface wrinkling at permissive temperatures (which persist even after recovery from sublethal freezing). This wrinkling is also reflected by F-actin staining (Fig. S7), and can be observed as wavy borders between cells in midsection images of SDA larvae (Figs S4 and S5). For representative images of fat body peripheral α-tubulin morphology in all 15 treatments, see Fig. S6.

Journal of Experimental Biology (2018) 221, jeb189647. doi:10.1242/jeb.189647

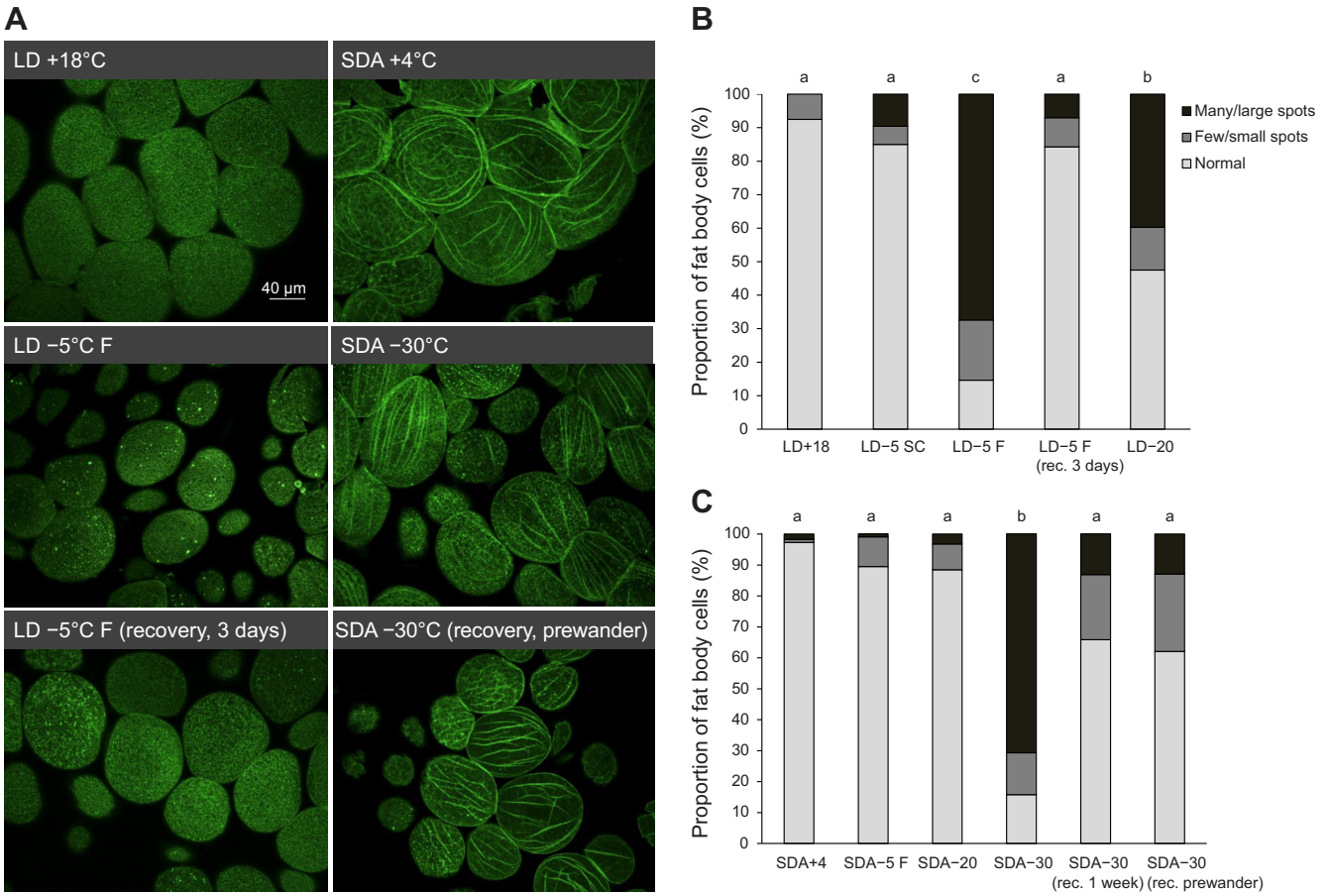

Fig. 4. F-actin aggregation near the fat body cell periphery in malt fly larvae before, immediately after and upon recovery from freezing (visualized by phalloidin staining, confocal microscopy). (A) Representative images of active, long-day-reared larvae (LD, freeze-intolerant; left panels) and diapausing, cold-acclimated larvae (SDA, extremely freeze tolerant; right panels). F-actin aggregated into brighter spots upon freezing at −5°C (LD larvae) or −30°C (SDA larvae), with most spots disappearing upon recovery. Note cell surface wrinkling, which is characteristic of all SDA larvae. The proportion of fat body cells with many and/or large spots (indicated by black portions of the bar graph) was quantified and compared among LD larvae (B) and among SDA larvae (C) by ANOVA (n=9–20 larvae, each with ∼3 technical replicate images per treatment). Different letters indicate significantly different (P<0.05) proportions of cells with many and/or large spots according to Tukey's HSD. LD larvae were imaged after 3 days of recovery (on account of rapid development and pupation), while slower-developing SDA larvae were imaged after 1 week of recovery and upon reaching the prewandering stage (approximately 3 weeks recovery). Representative images of F-actin morphology on the fat body surface for all 15 treatments are given in Fig. S6.

disruptions are seemingly without detriment. Below, we focus our discussion on the prominent fat body structural changes and their relationship to whole-animal mortality.

Lipid droplet coalescence

Coalescence of fat body lipid droplets upon freezing has been observed in other insects (Salt, 1962; Asahina, 1970; Lee et al., 1993) and, as in malt flies, this phenomenon appears to be primarily driven by temperature (Lee et al., 1993). The extent of lipid droplet coalescence was also modified by malt fly freeze-tolerance status: diapause and cold acclimation lowered the temperature of coalescence by 10°C. That this coalescence should become complete and persist in diapausing, cold-acclimated larvae upon recovery from sublethal freezing was unexpected. These larvae have good survival and emergence success (Rozsypal et al., 2018); therefore, droplet coalescence is clearly not a lethal form of freeze injury. Freeze-tolerant *Eurosta solidaginis* (Diptera) and *Cephus cinctus* (Hymenoptera) similarly survive such lipid coalescence in the fat body cells (Salt, 1962; Lee et al., 1993). It is therefore unclear whether protection of lipid droplet morphology to lower temperatures is somehow beneficial for diapausing, cold-acclimated malt fly larvae. Energy utilization problems stemming from such a substantial reduction in lipid droplet surface area could affect reproductive output or time to starvation, but these sublethal effects of freezing have yet to be determined for adults.

Loss of α-tubulin radial structure

Disintegration of fat body α-tubulin radial structure upon freezing was less substantial for diapausing, cold-acclimated malt fly larvae (a variant that also defended lipid droplet structure to lower temperatures), but it is unclear whether failure of tubulin upon freezing caused coalescence of lipid droplets or vice versa, or whether these effects simply coincide. Still, α-tubulin disruption is clearly also a non-lethal consequence of cold exposure, as recovered larvae did not repair α-tubulin structure. Although the fine mesh structure of α-tubulin on the fat cell periphery showed subtle differences among control, lethally frozen and recovered larvae, it is unclear whether these differences have functional consequences for the cells.

Surface wrinkling of fat body cells

Larval fat body cell surface wrinkling upon lethal freezing suggests freeze-attributed dehydration which could correspond with

Journal of Experimental Biology (2018) 221, jeb189647. doi:10.1242/jeb.189647

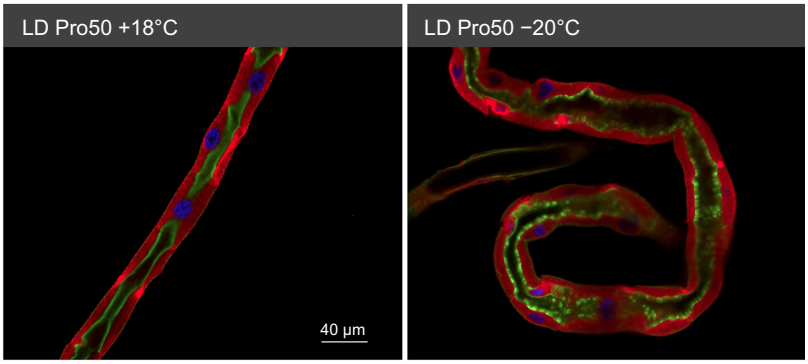

Fig. 5. Effect of freezing on F-actin morphology in the Malpighian tubules of long-day-reared (LD, non-diapausing) malt flies supplemented with dietary proline, imaged by confocal microscopy. No LD larvae survive to adulthood after being frozen at −20°C, while roughly 60% do survive such freezing if supplemented with 50 mg proline per 1 g diet (Pro50). Red: α-tubulin (anti-α-tubulin antibody), green: F-actin (phalloidin), blue: nuclei (DAPI). All Malpighian tubules of frozen LD Pro50 larvae (*n*=33 tubules across 10 larvae) exhibited lumenal F-actin aggregation, while none exhibited aggregation +18°C (*n*=31 tubules across 10 larvae). For representative Malpighian tubule images from all treatments, see Fig. S10.

mortality (Sinclair and Renault, 2010; Rozsypal et al., 2018). However, extensive cell wrinkling prior to freezing and following recovery in diapausing, cold-acclimated malt flies suggests that this physiological state provides some degree of protective intracellular dehydration. Such dehydration could both lower the risk of intracellular freezing and subsequently prevent rapid fluctuations in cell volume and osmolality associated with freeze–thaw. Still, survival of these extremely freeze-tolerant larvae is essentially independent of the body's ice fraction across a broad range of sub-zero temperatures (Rozsypal et al., 2018). Dehydration could therefore instead concentrate intracellular proline or other cryoprotectants to thresholds that promote macromolecular

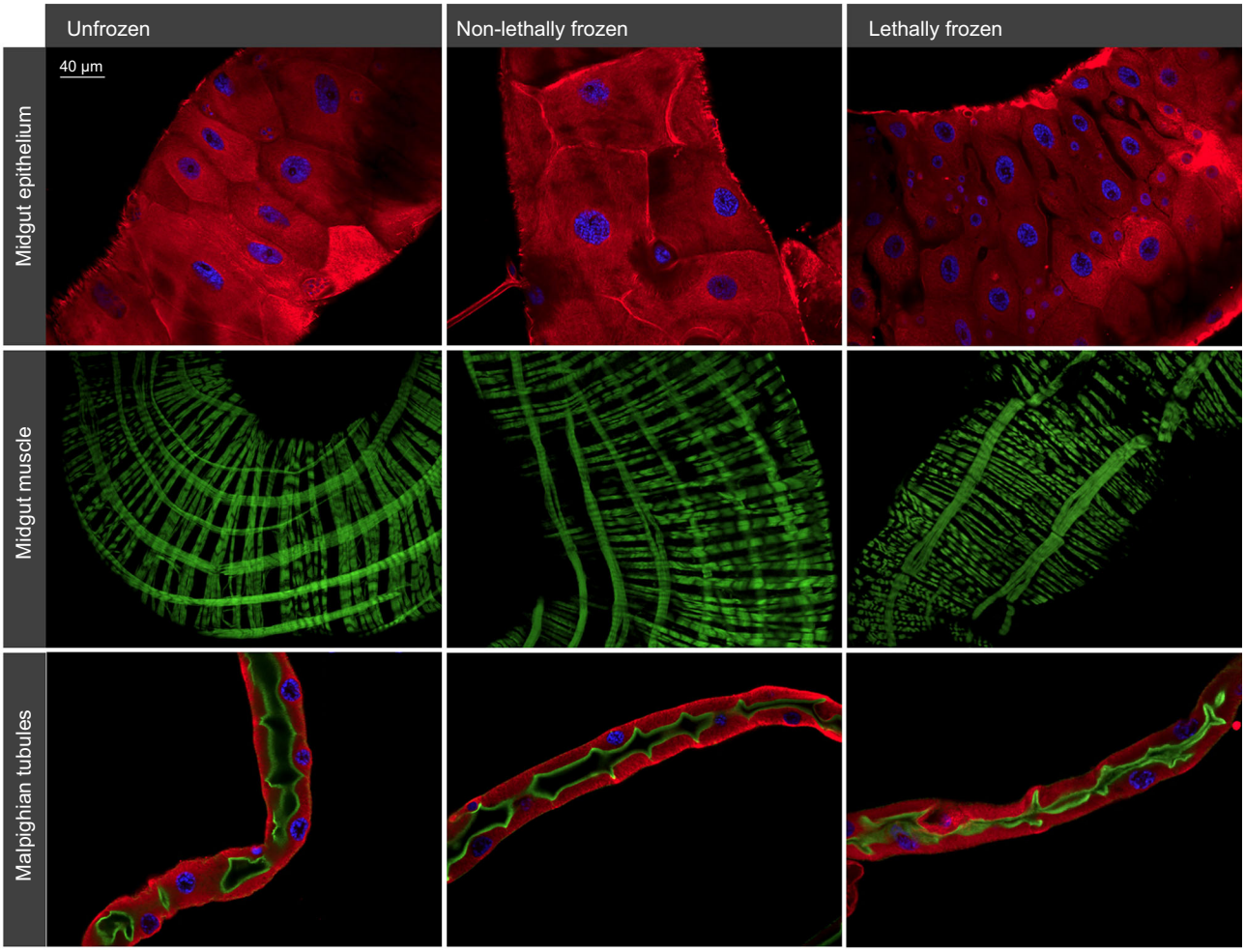

Fig. 6. Representative anterior midgut (muscle and epithelium) and Malpighian tubules of malt fly larvae after non-lethal and lethal freezing. With the exception of proline treatments (see Fig. 5), freezing generally had no discernible effect on F-actin or α-tubulin structure in these tissues. Red: α-tubulin (anti-α-tubulin antibody); green: F-actin (phalloidin); blue: nuclei (DAPI). Treatments shown here (from left to right): midgut epithelium: LD+18°C, LD−5°C F, LD−20°C; midgut muscle: LD−5°C SC, SDA−20°C, LD−20°C; Malpighian tubules: SDA+4°C, LD−5°C, SDA−20°C LN_2. LD: long-day-reared, non-acclimated, non-diapausing; SDA: short-day-reared, cold-acclimated, diapausing; F: frozen at −5°C; SC: not frozen at −5°C; LN_2: exposed to liquid nitrogen immediately after cooling to −20 or −30°C. Complete details about the acclimation and cold exposure treatments are given in Figs S1 and S2, respectively. For representative images of all 15 treatments, see Figs S8 (anterior midgut epithelia), S8 (anterior midgut muscle) and S10 (Malpighian tubules).

protection (Koštál et al., 2011a; Rozsypal et al., 2018), or perhaps precondition cells against anticipated osmotic stress. Alternatively, fat body dehydration could be a non-protective consequence of dormancy (Danks, 2000) and/or the cold acclimation regime (i.e. an effect of age and loss of body water over time).

Aggregation of F-actin

F-actin aggregation (spotting) at the periphery of fat body cells was modified by freeze tolerance status: diapause and cold acclimation lowered the temperature at which spots appeared by 25°C. We suspect that these apparent protein aggregates result from depolymerization of F-actin upon cold exposure (Kayukawa and Ishikawa, 2009), and that a reduction in the temperature at which actin aggregates form may indicate a general trend of protein stabilization at freezing temperatures. Disappearance of actin aggregates in the fat bodies of recovered larvae suggests that repair of the actin cytoskeleton may correlate with survival of a freezing challenge. Cold-acclimated malt flies indeed increase expression of genes involved in both protein stabilization (e.g. heat shock proteins) and degradation (e.g. ubiquitination and proteasome machinery; L.E.D.M. and V.K., unpublished data), and cytoskeletal protection appears to underlie cold acclimation in other insects (Kim et al., 2006; Kayukawa and Ishikawa, 2009) and plants (Örvar et al., 2000; Ouellet et al., 2001). However, it is impossible to determine whether lethally frozen malt flies perish owing to an inability to repair actin structure.

Anterior midgut and Malpighian tubule morphologies

Unlike in the fat body, the general morphologies and structural (cytoskeletal) appearance of the malt fly anterior midgut and Malpighian tubules were mostly unchanged among treatments. In the anterior midgut, neither the epithelium (visualized by α-tubulin staining) nor muscle (visualized by F-actin staining) differed between freeze tolerance status or upon a freezing challenge (whether lethal or sublethal). Although damage to muscle cell ultrastructure is visible in lethally frozen *Eurosta solidaginis* gall flies (Collins et al., 1997), such injury in malt fly muscle may not have been detectible via phalloidin staining and the lower magnification used here. Freeze injury in the gut may also not be immediately apparent upon thawing. We did observe some (albeit variable) freezing-associated F-actin aggregation in the Malpighian tubule lumen, which, like in the fat body, was apparently repaired by larvae during recovery. General Malpighian tubule morphology and α-tubulin structure were otherwise unaffected. Investigation of other structural components in these tissues (e.g. cell junctions; MacMillan et al., 2017) either immediately or some hours after a freezing challenge may uncover other forms of cryoinjury.

Effects of dietary proline and cryopreservation in LN_2

Dietary proline improves survival of warm-acclimated malt flies at −20°C from zero to roughly 50% (Rozsypal et al., 2018); therefore, it is unclear why we observed more pronounced actin aggregation in the fat body and Malpighian tubules of these larvae compared with non-supplemented larvae frozen to the same temperature. Pre-freeze surface wrinkling in some fat body cells of proline-supplemented larvae could have resulted from the osmotic effects of proline, and may therefore confer some form of protective pre-dehydration (discussed above). Because cell morphologies were similar after exposure to LN_2 regardless of whether larvae were pre-frozen at −20°C (resulting in poor larval survival and no metamorphosis to adults) or −30°C (allowing for substantial larval survival and adult metamorphosis for ca. 40% of individuals), it is likely that the mechanisms conferring extreme freeze tolerance (e.g. glass transition of body liquids; Rozsypal et al., 2018) cause no detectable morphological changes in the structures and at the scale visualized presently.

Conclusions

Uncovering freeze-attributed damages that correlate with insect mortality remains a challenge, but the freeze-susceptible fat body and (to some degree) Malpighian tubules of malt fly larvae appear to be suitable indicators of cryoinjury. Our observations suggest that repair or removal of damaged (aggregated) cytoskeletal proteins is a promising avenue of further investigation for the mechanisms of acquired freeze tolerance, and we expect that macromolecule protection and repair may be a general feature of cold-acclimated insects. We therefore recommend similar morphological (and ultrastructural) assessments of the effects of acclimation and freezing on other macromolecules and cell features (e.g. cell junctions and mitochondria; Collins et al., 1997). Cellular pre-dehydration – which may protect cells from osmotic cryoinjury – is another potential mechanism of acquired freeze tolerance that warrants future consideration. We show that fat body lipid droplet coalescence is not an injury associated with freeze mortality, but we recommend rigorous assessment of any sublethal effects that this coalescence may cause in adults.

Acknowledgements

We would like to thank Jaroslava Korbelová for malt fly rearing and cold exposure, Irena Vacková for malt fly colony maintenance and Hana Sehadová for confocal microscopy assistance.

Competing interests

The authors declare no competing or financial interests.

Author contributions

Conceptualization: L.E.D.M., V.K.; Methodology: L.E.D.M.; Validation: L.E.D.M.; Formal analysis: L.E.D.M.; Investigation: L.E.D.M.; Resources: V.K.; Data curation: L.E.D.M.; Writing - original draft: L.E.D.M.; Writing - review & editing: L.E.D.M., V.K.; Visualization: L.E.D.M., T.S.; Supervision: V.K.; Project administration: L.E.D.M., V.K.; Funding acquisition: V.K.

Funding

This research was supported by the Czech Science Foundation (Grantová Agentura České Republiky grant 16–06374 S) to V.K.

Data availability

All image data are available upon request.

Supplementary information

Supplementary information available online at
http://jeb.biologists.org/lookup/doi/10.1242/jeb.189647.supplemental

References

Asahina, E. (1970). Frost resistance in insects. *Adv. In Insect Phys.* **6**, 1-49.

Ayrinhac, A., Debat, V., Gibert, P., Kister, A.-G., Legout, H., Moreteau, B., Vergilino, R. and David, J. R. (2004). Cold adaptation in geographical populations of *Drosophila melanogaster*: phenotypic plasticity is more important than genetic variability. *Funct. Ecol.* **18**, 700-706.

Ayvaz, A., Karasu, E., Karabörklü, S. and Tunçbilek, A. Ş. (2008). Effects of cold storage, rearing temperature, parasitoid age and irradiation on the performance of *Trichogramma evanescens* Westwood (Hymenoptera: Trichogrammatidae). *J. Stored Prod. Res.* **44**, 232-240.

Belous, A. (1992). The role of regulatory systems modulating the state of cytoskeletal proteins under the temperature and osmotic effects. *Problems Cryobiol.* **4**, 3-14.

Bhatnagar, B. S., Bogner, R. H. and Pikal, M. J. (2007). Protein stability during freezing: separation of stresses and mechanisms of protein stabilization. *Pharm. Dev. Technol.* **12**, 505-523.

Bloem, S., Carpenter, J. E. and Dorn, S. (2006). Mobility of mass-reared diapaused and nondiapaused *Cydia pomonella* (Lepidoptera: Tortricidae): effect of mating status and treatment with gamma radiation. *J. Econ. Entomol.* **99**, 699-706.

Clark, M. S. and Worland, M. R. (2008). How insects survive the cold: molecular mechanisms—a review. *J. Comp. Physiol. B* **178**, 917-933.
Colinet, H. and Boivin, G. (2011). Insect parasitoids cold storage: a comprehensive review of factors of variability and consequences. *Biol. Control* **58**, 83-95.
Collins, S. D., Allenspach, A. L. and Lee, R. E., Jr. (1997). Ultrastructural effects of lethal freezing on brain, muscle and Malpighian tubules from freeze-tolerant larvae of the gall fly, *Eurosta solidaginis*. *J. Insect Physiol.* **43**, 39-45.
Cottam, D. M., Tucker, J. B., Rogers-Bald, M. M., Mackie, J. B., Macintyre, J., Scarborough, J. A., Ohkura, H. and Milner, M. J. (2006). Non-centrosomal microtubule-organising centres in cold-treated cultured *Drosophila* cells. *Cell Motil. Cytoskelet.* **63**, 88-100.
Danks, H. V. (2000). Dehydration in dormant insects. *J. Insect Physiol.* **46**, 837-852.
Des Marteaux, L. E., Stinziano, J. R. and Sinclair, B. J. (2018). Effects of cold acclimation on rectal macromorphology, ultrastructure, and cytoskeletal stability in *Gryllus pennsylvanicus* crickets. *J. Insect Physiol.* **104**, 15-24.
Dias, C. L., Ala-Nissila, T., Wong-ekkabut, J., Vattulainen, I., Grant, M. and Karttunen, M. (2010). The hydrophobic effect and its role in cold denaturation. *Cryobiology* **60**, 91-99.
Gerken, A. R., Eller, O. C., Hahn, D. A. and Morgan, T. J. (2015). Constraints, independence, and evolution of thermal plasticity: probing genetic architecture of long- and short-term thermal acclimation. *Proc. Natl Acad. Sci. USA* **112**, 4399-4404.
Ghazy, N. A., Suzuki, T., Shah, M., Amano, H. and Ohyama, K. (2012). Effect of long-term cold storage of the predatory mite *Neoseiulus californicus* at high relative humidity on post-storage biological traits. *BioControl* **57**, 635-641.
Gosden, R. (2011). Cryopreservation: a cold look at technology for fertility preservation. *Fertil. Steril.* **96**, 264-268.
Hazel, J. R. (1995). Thermal adaptation in biological membranes: is homeoviscous adaptation the explanation? *Annu. Rev. Physiol.* **57**, 19-42.
Hochachka, P. and Somero, G. (2002). *Biochemical Adaptation. Mechanism and Process in Physiological Evolution*. Oxford University Press.
Izumi, Y., Sonoda, S., Yoshida, H. and Tsumuki, H. (2005). Identification of tissues showing the lowest tolerance to freezing in larvae of the rice stem borer, *Chilo suppressalis*. *Physiol. Entomol.* **30**, 324-331.
Kayukawa, T. and Ishikawa, Y. (2009). Chaperonin contributes to cold hardiness of the onion maggot *Delia antiqua* through repression of depolymerization of actin at low temperatures. *PLoS ONE* **4**, e8277.
Kim, M., Robich, R. M., Rinehart, J. P. and Denlinger, D. L. (2006). Upregulation of two actin genes and redistribution of actin during diapause and cold stress in the northern house mosquito, *Culex pipiens*. *J. Insect Physiol.* **52**, 1226-1233.
Koštál, V. R., Berková, P. and Šimek, P. (2003). Remodelling of membrane phospholipids during transition to diapause and cold-acclimation in the larvae of *Chymomyza costata* (Drosophilidae). *Comp. Biochem. Physiol. B* **135**, 407-419.
Koštál, V., Korbelová, J., Rozsypal, J., Zahradníčková, H., Cimlová, J., Tomčala, A. and Šimek, P. (2011a). Long-term cold acclimation extends survival time at 0°C and modifies the metabolomic profiles of the larvae of the fruit fly *Drosophila melanogaster*. *PLoS ONE* **6**, e25025.
Koštál, V., Zahradníčková, H. and Šimek, P. (2011b). Hyperprolinemic larvae of the drosophilid fly, *Chymomyza costata*, survive cryopreservation in liquid nitrogen. *Proc. Natl Acad. Sci. USA* **108**, 13041-13046.
Koštál, V., Šimek, P., Zahradníčková, H., Cimlová, J. and Štětina, T. (2012). Conversion of the chill susceptible fruit fly larva (*Drosophila melanogaster*) to a freeze tolerant organism. *Proc. Natl Acad. Sci. USA* **109**, 3270-3274.
Koštál, V., Mollaei, M. and Schöttner, K. (2016). Diapause induction as an interplay between seasonal token stimuli, and modifying and directly limiting factors: hibernation in *Chymomyza costata*. *Physiol. Entomol.* **41**, 344-357.
Kvist, J., Wheat, C. W., Kallioniemi, E., Saastamoinen, M., Hanski, I. and Frilander, M. J. (2013). Temperature treatments during larval development reveal extensive heritable and plastic variation in gene expression and life history traits. *Mol. Ecol.* **22**, 602-619.
Lee, R. E., McGrath, J. J., Morason, R. T. and Taddeo, R. M. (1993). Survival of intracellular freezing, lipid coalescence and osmotic fragility in fat body cells of the freeze-tolerant gall fly *Eurosta solidaginis*. *J. Insect Physiol.* **39**, 445-450.
Leopold, R. A. (1991). Cryopreservation of insect germplasm: cells, tissues and organisms. In *Insects at Low Temperature* (ed. R. E. Lee Jr and D. L. Denlinger), pp. 379-407. Springer.
Leopold, R. (2007). Colony maintenance and mass-rearing: using cold storage technology for extending the shelf-life of insects. In *Area-wide Control of Insect Pests* (ed. M. J. B. Vreysen, A. S. Robinson and J. Hendrichs), pp. 149-162. Springer.
Li, N. G. (2016). Strong tolerance to freezing is a major survival strategy in insects inhabiting central Yakutia (Sakha Republic, Russia), the coldest region on earth. *Cryobiology* **73**, 221-225.
MacMillan, H. A., Yerushalmi, G. Y., Jonusaite, S., Kelly, S. P. and Donini, A. (2017). Thermal acclimation mitigates cold-induced paracellular leak from the *Drosophila* gut. *Sci. Rep.* **7**, 8807.
Marshall, K. E. and Sinclair, B. J. (2011). The sub-lethal effects of repeated freezing in the woolly bear caterpillar *Pyrrharctia isabella*. *J. Exp. Biol.* **214**, 1205-1212.
McKinnon, A. H. (2015). Freeze tolerance in the spring field cricket, *Gryllus veletis*. MSc thesis, *Department of Biology*, The University of Western Ontario.
Michaud, M. R. and Denlinger, D. L. (2004). Molecular modalities of insect cold survival: current understanding and future trends. *Int. Congr. Ser.* **1275**, 32-46.
Minton, A. P. (2000). Implications of macromolecular crowding for protein assembly. *Curr. Opin. Struct. Biol.* **10**, 34-39.
Moon, I., Fujikawa, S. and Shimada, K. (1996). Cryopreservation of *Chymomyza* larvae (Diptera: Drosophilidae) at –196°C with extracellular freezing. *CryoLetters* **17**, 105-110.
Neufeld, D. S. and Leader, L. P. (1998). Freezing survival by isolated Malpighian tubules of the New Zealand alpine weta *Hemideina maori*. *J. Exp. Biol.* **201**, 227-236.
Örvar, B. L., Sangwan, V., Omann, F. and Dhindsa, R. S. (2000). Early steps in cold sensing by plant cells: the role of actin cytoskeleton and membrane fluidity. *Plant J.* **23**, 785-794.
Ouellet, F., Carpentier, É., Cope, M. J. T. V., Monroy, A. F. and Sarhan, F. (2001). Regulation of a wheat actin-depolymerizing factor during cold acclimation. *Plant Physiol.* **125**, 360-368.
Pegg, D. E. (2007). Principles of cryopreservation. In *Cryopreservation and Freeze-Drying Protocols* (ed. J. G. Day and G. N. Stacey), pp. 39-57. Springer.
Pegg, D. E. (2015). Principles of cryopreservation. In *Cryopreservation and Freeze-Drying Protocols* (ed. W. F. Wolkers and H. Oldenhof), pp. 3-19. Springer.
Ramløv, H. and Westh, P. (1992). Survival of the cryptobiotic eutardigrade *Adorybiotus coronifer* during cooling to –196°C: effect of cooling rate, trehalose level, and short-term acclimation. *Cryobiology* **29**, 125-130.
Riihimaa, A. J. and Kimura, M. T. (1988). A mutant strain of *Chymomyza costata* (Diptera: Drosophilidae) insensitive to diapause-inducing action of photoperiod. *Physiol. Entomol.* **13**, 441-445.
Rozsypal, J., Moos, M., Šimek, P. and Koštál, V. (2018). Thermal analysis of ice and glass transitions in insects that do and do not survive freezing. *J. Exp. Biol.* **221**, jeb170464.
Russotti, G., Campbell, J., Toner, M. and Yarmush, M. L. (1997). Studies of heat and PGA1-induced cold tolerance show that HSP27 may help preserve actin morphology during hypothermia. *Tissue Eng.* **3**, 135-147.
Salt, R. W. (1962). Intracellular freezing in insects. *Nature* **193**, 1207.
Sformo, T., Walters, K., Jeannet, K., Wowk, B., Fahy, G. M., Barnes, B. M. and Duman, J. G. (2010). Deep supercooling, vitrification and limited survival to –100° C in the Alaskan beetle *Cucujus clavipes puniceus* (Coleoptera: Cucujidae) larvae. *J. Exp. Biol.* **213**, 502-509.
Sgrò, C. M., Terblanche, J. S. and Hoffmann, A. A. (2016). What can plasticity contribute to insect responses to climate change? *Annu. Rev. Entomol.* **61**, 433-451.
Sinclair, B. J. and Renault, D. (2010). Intracellular ice formation in insects: unresolved after 50 years? *Comp. Biochem. Physiol. A* **155**, 14-18.
Sinclair, B. J., Addo-Bediako, A. and Chown, S. L. (2003). Climatic variability and the evolution of insect freeze tolerance. *Biol. Rev.* **78**, 181-195.
Štětina, T., Hůla, P., Moos, M., Šimek, P., Šmilauer, P. and Koštál, V. (2018). Recovery from supercooling, freezing, and cryopreservation stress in larvae of the drosophilid fly, *Chymomyza costata*. *Sci. Rep.* **8**, 4414.
Storey, K. B. and Storey, J. M. (2012). Insect cold hardiness: metabolic, gene, and protein adaptation. *Can. J. Zool.* **90**, 456-475.
Suzuki, D., Miyamoto, T., Kikawada, T., Watanabe, M. and Suzuki, T. (2014). A leech capable of surviving exposure to extremely low temperatures. *PLoS ONE* **9**, e86807.
Teets, N. M., Kawarasaki, Y., Lee, R. E. and Denlinger, D. L. (2011). Survival and energetic costs of repeated cold exposure in the Antarctic midge, *Belgica antarctica*: a comparison between frozen and supercooled larvae. *J. Exp. Biol.* **214**, 806-814.
Teets, N. M., Peyton, J. T., Ragland, G. J., Colinet, H., Renault, D., Hahn, D. A. and Denlinger, D. L. (2012). Combined transcriptomic and metabolomic approach uncovers molecular mechanisms of cold tolerance in a temperate flesh fly. *Physiol. Genomics* **44**, 764-777.
Toxopeus, J. and Sinclair, B. J. (2018). Mechanisms underlying insect freeze tolerance. *Biol. Rev.* **93**, 1891-1914.
Van Wyk, J., Gerber, H. and Van, W. A. (1977). Cryopreservation of the infective larvae of the common nematodes of ruminants. *Onderstepoort J. Vet. Res.* **44**, 173-194.
Worland, M. R., Wharton, D. A. and Byars, S. G. (2004). Intracellular freezing and survival in the freeze tolerant alpine cockroach *Celatoblatta quinquemaculata*. *J. Insect Physiol.* **50**, 225-232.

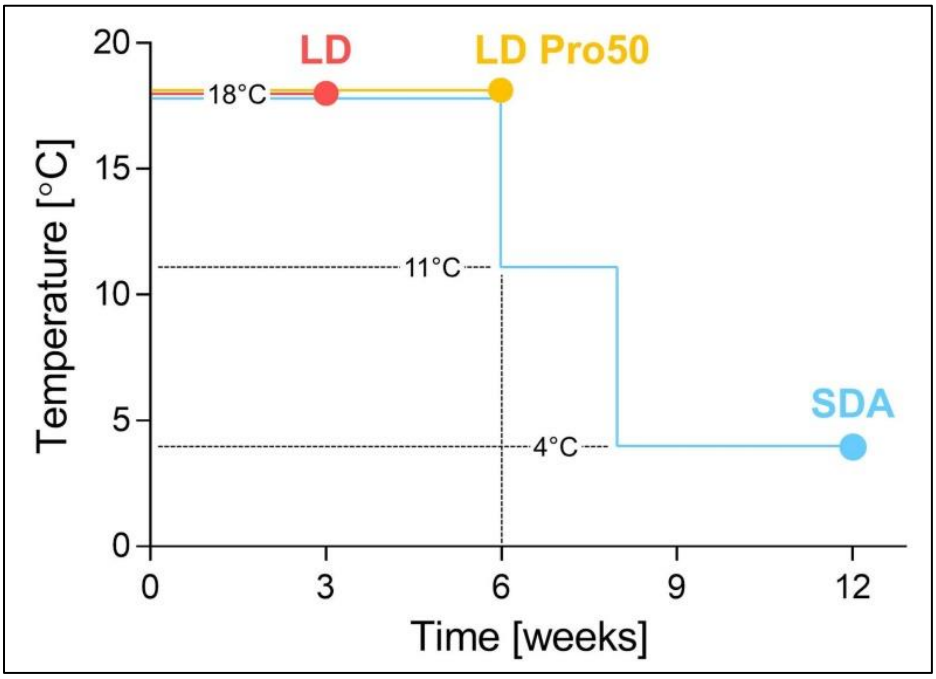

Figure S1. Acclimation of *Chymomyza costata* larvae.

The larvae were reared under constant 18°C and two different photoperiods (LD and SD). Under long day length (LD, 16 h/8 h light/dark cycle) the larvae continue direct development (to pupariation) but under short day length (SD, 12 h/12 h light/dark cycle) they enter diapause (hormonally regulated developmental arrest) (Koštál et al., 2000 **JIP**, 2016 **PE**). **LD**, long day-reared, non-diapause, warm-acclimated larvae in the late 3rd instar (pre-wandering); **LD Pro50**, same as LD but fed L-proline-augmented diet (50 mg of L-proline added per g of diet), which delays their development; **SDA**, cold-acclimated (under constant darkness), diapausing larvae, which spontaneously accumulate large amounts of L-proline in their body. Both treatments, LD Pro50 and SDA, result in dramatic increase of freeze tolerance according to our previous studies (Koštál et al., 2012 **PNAS**; Rozsypal et al. 2018 **JEB**).

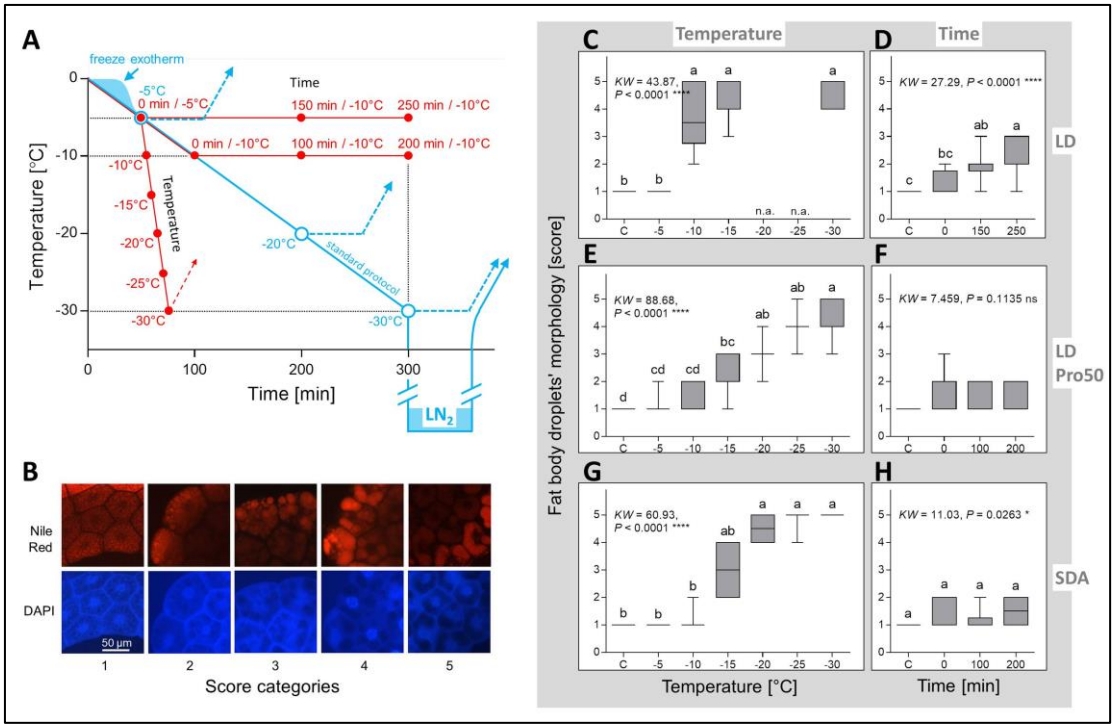

Figure S2. Freezing protocol and lipid droplet coalescence in the fat body of *Chymomyza costata* larvae exposed to cold stress. Fluorescence microscopy.

(**A**) Shows standard freezing and cryopreservation protocol (blue line) (according to Rozsypal et al., 2018 **JEB**) and also the specific protocols used to assess the effects of either low temperatures or time spent at -5°C or -10°C on lipid droplet coalescence (red lines). All larvae were inoculated by external ice crystals and frozen at relatively high subzero temperature (freeze exotherm). The cooling rate was set to 0.1°C min^{-1} in programmable Ministat 240 circulator (Huber, Offenburg, Germany). **Standard protocol:** blue empty circles show three temperatures (-5, -20, and -30°C) to which the larvae were cooled and then, after spending 1 hour at the target temperature, heated to +5°C (0.6°C min^{-1}), dissected and processed for confocal or TEM microscopy. Some SDA larvae, pre-frozen to -30°C, were plunged to liquid nitrogen (LN_2) for 1h. **The effect of low temperatures:** larvae were rapidly (1°C min^{-1}) cooled from -5°C to different target temperatures ranging between -10 and -30°C. Immediately after reaching the target temperature, the heating step started and the melted larvae were immediately processed for fluorescence microscopy observation. **The effect of time:** after reaching -5°C (LD) or -10°C (LD Pro50, SDA), the larvae were maintained at the target temperature for up to 250 min, then heated and processed for fluorescence microscopy.

(**B**) Immediately upon melting, fat body was dissected in PBS (8.0 g NaCl; 0.2 g KCl; 1.8 g $Na_2HPO_4.2H_2O$; 0.24 g KH_2PO_4 in 800 mL water, set pH to 7.4, fill up to 1L), placed on microscopic slide (Superfrost Plus, Thermo Scientific), and covered with 40 µl of Nile Red (Sigma) working solution (WS). The WS was prepared fresh daily by, first, diluting the Nile Red stock (5% in DMSO) 1:50,000 with PBS:glycerol (1:1) solution, and second, adding 1/5 volume (40 µl to 200 µl) of ProLong Gold antifade reagent with DAPI (Molecular Probes, Life Technologies). The fat bodies (five per slide) were covered with cover slips and incubated at room temperature for 15 min (protected from light). Next, the fat body cells were photographed under Karl Zeiss Axioplan 2 fluorescence microscope using Cy3 (red, Nile Red signal) and DAPI (blue signal) filters. The coalescence of lipid droplets in each fat body was arbitrarily scored to five categories from 1 (normal state, no coalescence) to 5 (full coalescence) according to scale shown in (B).

(**C**) Results of lipid droplets coalescence scoring in larvae acclimated according to LD, LD Pro50, and SDA protocols (see Fig. S1). Each box shows 25 and 75 percentiles and median value (horizontal bar in the box), whiskers represent min and max values. Scores were taken from 15 fat bodies (three microscopic slides). The differences between boxes were assessed using Kruskal-Wallis rank test (*KW* statistics is shown) followed by Dunn's multiple comparisons test. The columns flanked by different letters are significantly different.

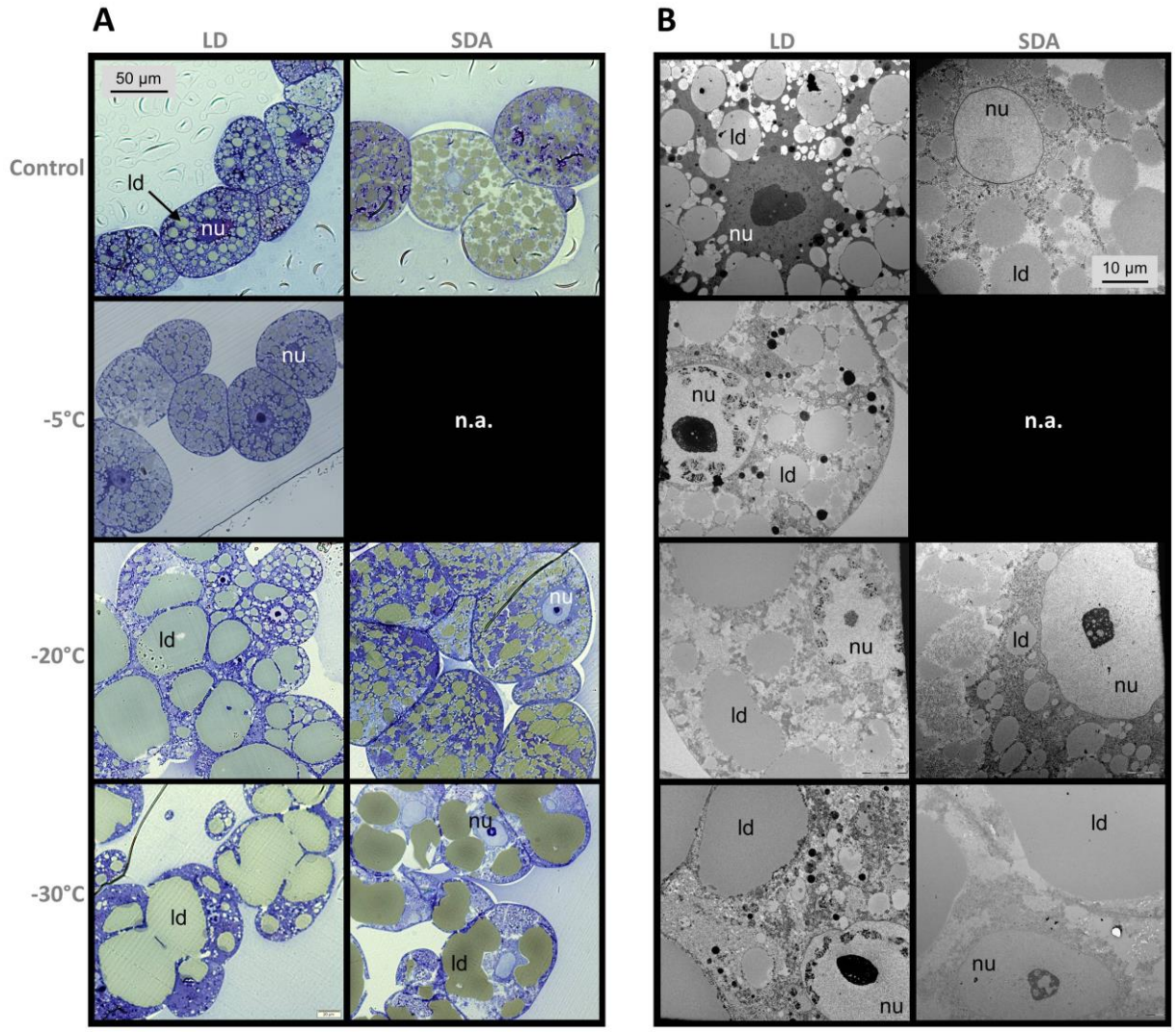

Figure S3. Lipid droplet coalescence in the fat body of *Chymomyza costata* larvae exposed to cold stress. Transmission electron microscopy (TEM).

The larvae acclimated to LD or SDA (see Fig. S1) were frozen to different target temperatures (-5, -20, and -30°C) using standard freezing protocol (see Fig. S2 A, blue line) and, upon melting, dissected and processed for TEM observation. (**A**) semi-thin sections (0.5 µm). The scale bar shown in upper left corner applies to all micrographs in the panel), (**B**) ultra-thin sections (70 nm). The scale bar shown in upper right corner applies to all micrographs in the panel). nu, nucleus; ld, lipid droplet.

Processing of fat body tissue for TEM: Fat bodies were dissected (under ice-cold PBS) into 1.5 mL microvials containing 500 µL of 2.5% glutaraldehyde in PBS. Tissues were fixed overnight, then embedded in 2% agarose gel for easier manipulation, washed in PBS (3 x 15 min), fixed in 2% OsO_4 (EMS, Hatfield, Pennsylvania) in PBS for 2 h, and finally washed in PBS (3 x 15 min). The samples were then dehydrated using grading acetone solutions (30%, 50%, 70%, 80%, 90%, 95%, 100%) in 15 min intervals. Dehydrated samples were saturated by grading solutions of resin Embed-812 (EMS, Hatfield, Pennsylvania) mixed with 100% acetone (resin:acetone at 1:2, 1:1, and 2:1 ratio, respectively) in 1 h intervals, then transferred into pure resin for 24 hours in desiccator. After complete dehydration, the samples were embedded in silicone forms containing pure resin and left for another 24 hours in 60°C for polymerization. Resin blocks containing fat body samples were sectioned using ultramicrotome Leica UC6 (Leica microsystems GmbH, Wetzlar, Germany) using DiATOME diamond knife (EMS, Hatfield, Pennsylvania). **The semithin sections** (500 nm) were placed in a droplet of 10% acetone on 24 x 60 mm glass slides, left on heater at 40°C

until dry, and then left in r.t. overnight for perfect drying. The semithin sections were stained by 1% Toluidine Blue (Sigma-Aldrich, Saint Luis, MO, USA) for 3-5 min and micrographs were taken by a bright-field microscope, Zeiss Axioplane 2 (Carl Zeiss Microscopy GmbH, Jena, Germany). **The ultrathin sections** (70 nm) were placed on 300-mesh-Cu grids. The samples were counter-stained by saturated ethanolic uranyl acetate for 30 min, followed by lead citrate for 20 min. The grids with sections were then coated by carbon film using JEOL JE 4C coater (JEOL, Tokio, Japan) and micrographs were taken by a transmission electron microscope, JEOL JEM - 1010 1 (JEOL, Tokio, Japan).

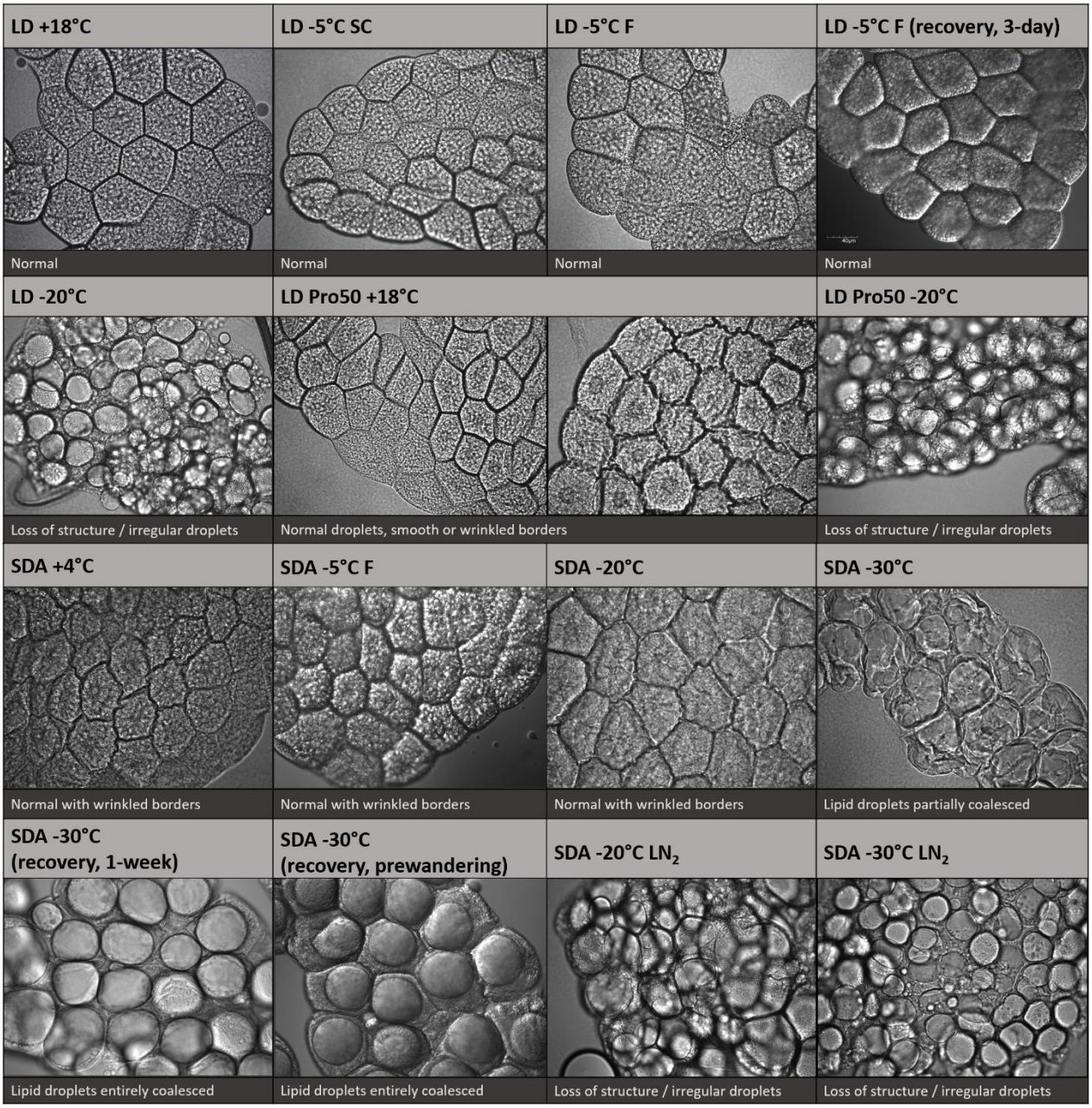

Figure S4. Representative brightfield images of *Chymomyza costata* larval fat bodies for all freeze tolerance variants and treatments, indicating extent of lipid droplet coalescence and cell border morphology (confocal microscopy).

LD: long-day reared, active variant, SDA: diapausing, cold-acclimated variant, Pro50: LD larvae supplemented with 50 mg proline per g diet, SC: larvae supercooled to -5°C without freezing, F: larvae frozen at -5°C. Larvae were cooled gradually and held at target temperatures for 1 hour before rewarming (details in Figure S2). Tissues were dissected and fixed immediately after cold treatments. Larvae exposed to LN_2 were first pre-frozen to either -20°C or -30°C. Prewandering SDA larvae had recovered for approximately 3 weeks.

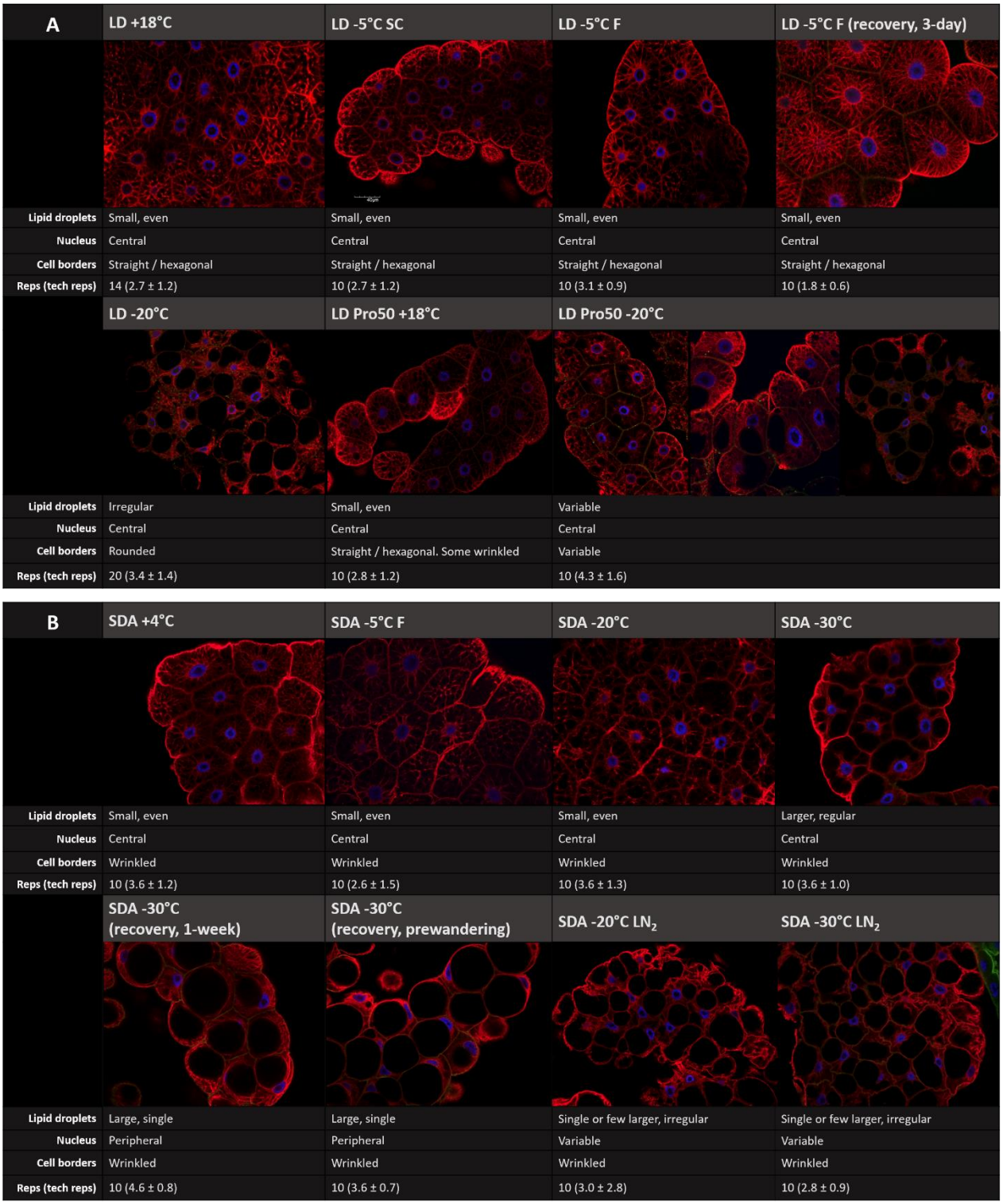

Figure S5. Representative fat body mid-section images for *Chymomyza costata* larvae of all freeze tolerance variants and treatments, indicating the extent of lipid droplet coalescence, cell border morphology, and α-tubulin radial structure (confocal microscopy).

A: LD - long-day reared, active variant, B: SDA - diapausing, cold-acclimated variant. LD Pro50 – LD larvae supplemented with 50 mg proline per g diet, SC: larvae supercooled to -5°C without freezing, F: larvae frozen at -5°C.

Larvae were cooled gradually and held at target temperatures for 1 hour before rewarming (details in Figure S2). Tissues were dissected, fixed, and stained immediately after cold treatments. Larvae exposed to LN_2 were first pre-frozen to either -20°C or -30°C. Prewandering SDA larvae had recovered for approximately 3 weeks. Red: α-tubulin (anti-α-tubulin antibody), green: F-actin (phalloidin, generally not visible), blue: nuclei (DAPI). Biological replication (number of larvae) and technical replication (mean ± s.e.m. fat body tissues imaged per larva) are indicated below each image.

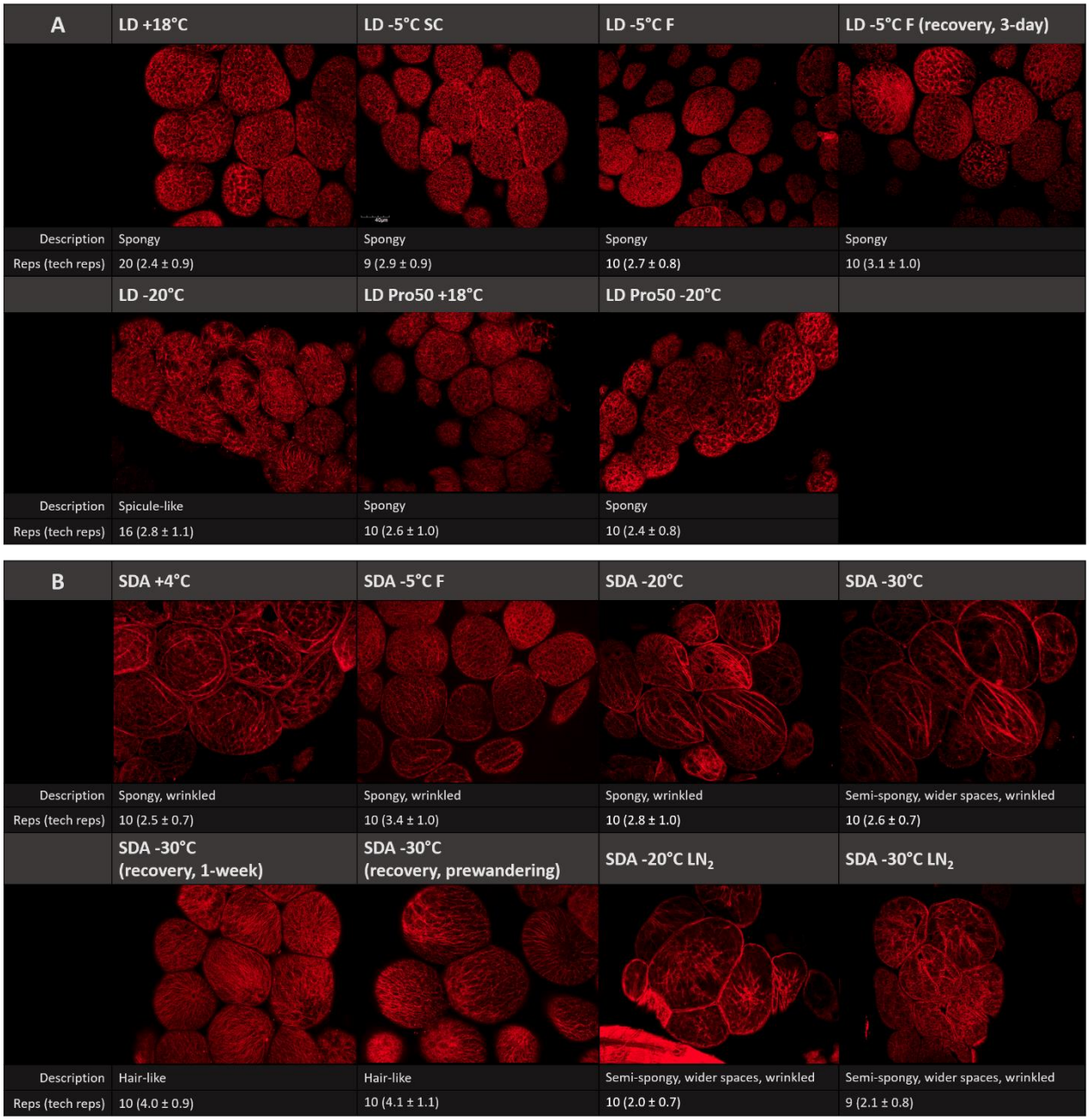

Figure S6. Representative *Chymomyza costata* larval fat body surface images for all freeze tolerance variants and treatments, indicating cell border morphology and α-tubulin radial structure (stained by anti-α-tubulin antibody, confocal microscopy).

A: LD - long-day reared, active variant, B: SDA - diapausing, cold-acclimated variant. LD Pro50 – LD larvae supplemented with 50 mg proline per g diet, SC: larvae supercooled to -5°C without freezing, F: larvae frozen at -5°C. Larvae were cooled gradually and held at target temperatures for 1 hour before rewarming (details in Figure S2). Tissues were dissected, fixed, and stained immediately after cold treatments. Larvae exposed to LN_2 were first pre-frozen to either -20°C or -30°C. Prewandering SDA larvae had recovered for approximately 3 weeks. Biological replication (number of larvae) and technical replication (mean ± s.e.m. fat body tissues imaged per larva) are indicated below each image.

Journal of Experimental Biology • Supplementary information

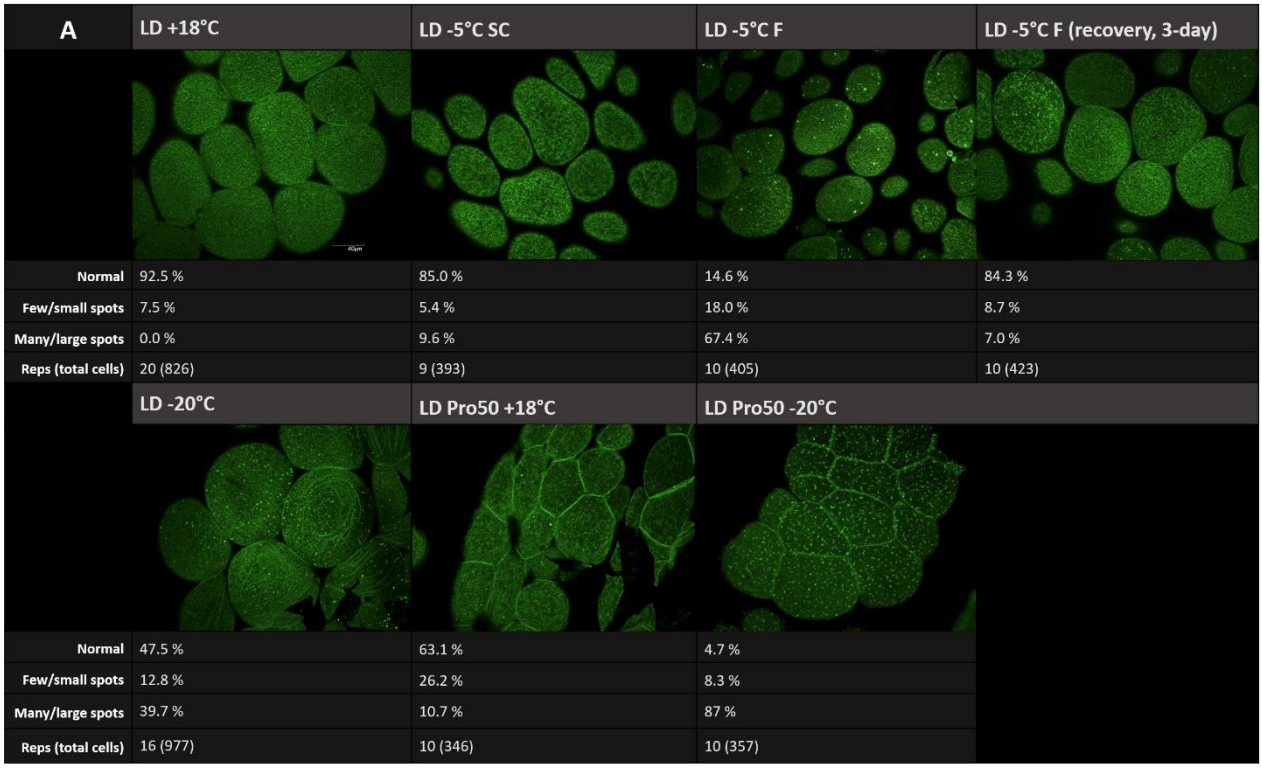

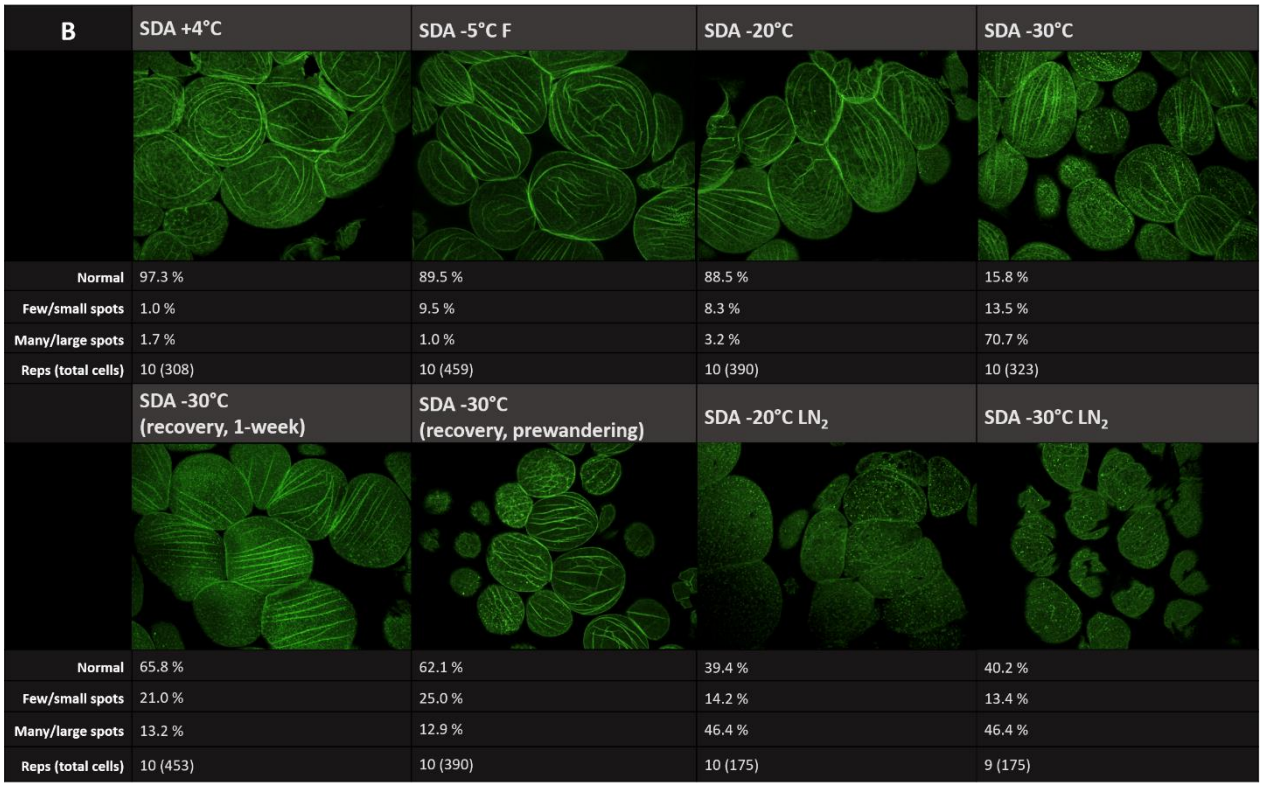

Figure S7. Representative *Chymomyza costata* larval fat body surface images for all freeze tolerance variants and treatments, indicating cell border and F-actin morphology (stained by phalloidin, confocal microscopy).

A: LD - long-day reared, active variant, B: SDA - diapausing, cold-acclimated variant. LD Pro50 – LD larvae supplemented with 50 mg proline per g diet, SC: larvae supercooled to -5°C without freezing, F: larvae frozen at -5°C. Larvae were cooled gradually and held at target temperatures for 1 hour before rewarming (details in Figure S2). Tissues were dissected, fixed, and stained immediately after cold treatments. Larvae exposed to LN_2 were first pre-frozen to either -20°C or -30°C. Prewandering SDA larvae had recovered for approximately 3 weeks. Biological replication (number of larvae) and technical replication (total number of fat body cells assessed across all biological replicates) are indicated below each image.

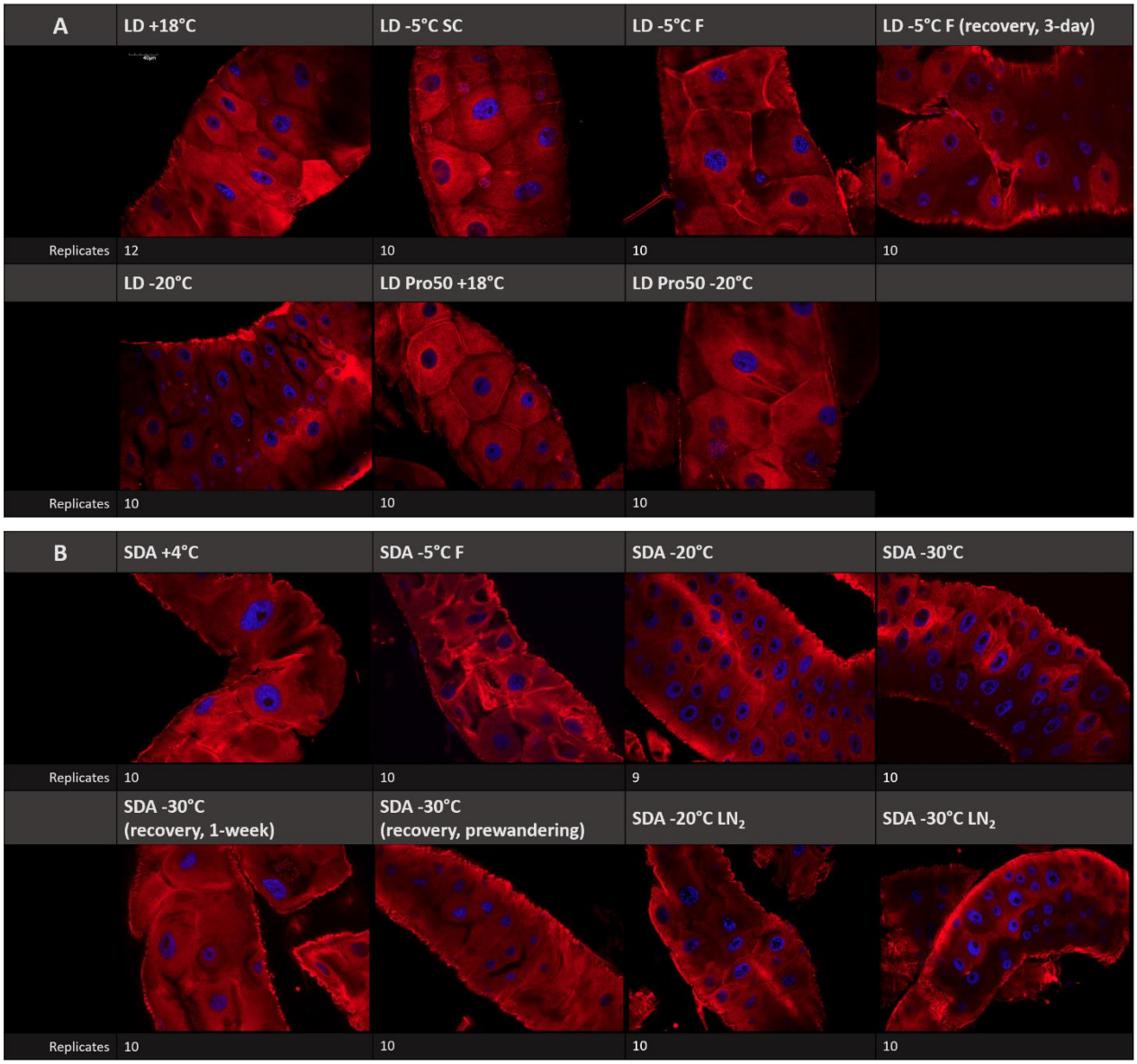

Figure S8. Representative *Chymomyza costata* larval anterior midgut epithelia for all freeze tolerance variants and treatments (confocal microscopy).

A: LD - long-day reared, active variant, B: SDA - diapausing, cold-acclimated variant. LD Pro50 – LD larvae supplemented with 50 mg proline per g diet, SC: larvae supercooled to -5°C without freezing, F: larvae frozen at -5°C. Larvae were cooled gradually and held at target temperatures for 1 hour before rewarming (details in Figure S2). Tissues were dissected, fixed, and stained immediately after cold treatments. Larvae exposed to LN_2 were first pre-frozen to either -20°C or -30°C. Prewandering SDA larvae had recovered for approximately 3 weeks. Red: α-tubulin (anti-α-tubulin antibody), blue: nuclei (DAPI). The biological replication (number of larvae) is indicated below each image.

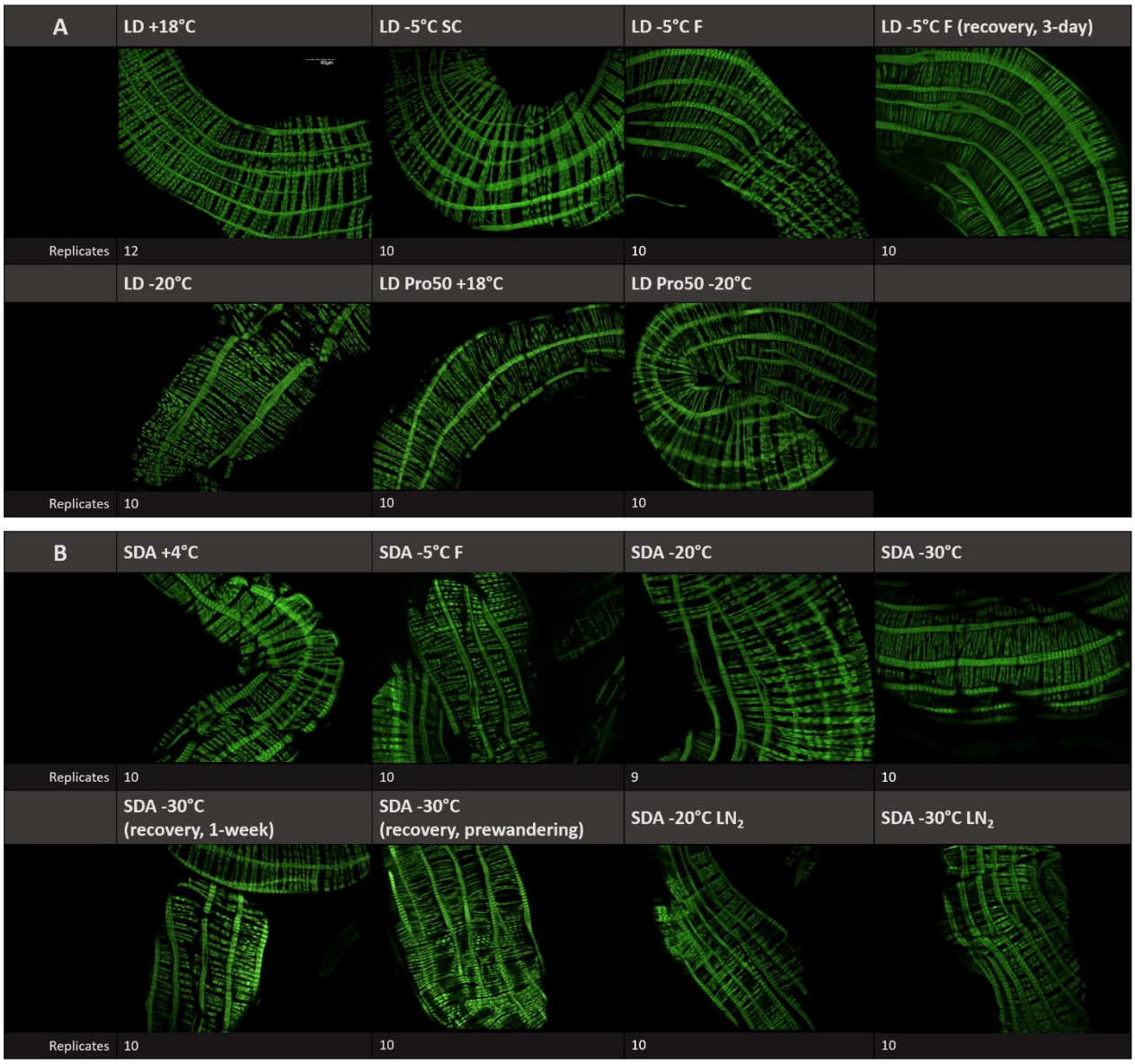

Figure S9. Representative *Chymomyza costata* larval anterior midgut muscle for all freeze tolerance variants and treatments (visualized by F-actin staining with phalloidin, confocal microscopy).

A: LD - long-day reared, active variant, B: SDA - diapausing, cold-acclimated variant. LD Pro50 – LD larvae supplemented with 50 mg proline per g diet, SC: larvae supercooled to -5°C without freezing, F: larvae frozen at -5°C. Larvae were cooled gradually and held at target temperatures for 1 hour before rewarming (details in Figure S2). Tissues were dissected, fixed, and stained immediately after cold treatments. Larvae exposed to LN_2 were first pre-frozen to either -20°C or -30°C. Prewandering SDA larvae had recovered for approximately 3 weeks. Biological replication (number of larvae) is indicated below each image.

Figure S10. Representative Malpighian tubules from *Chymomyza costata* larvae of all freeze tolerance variants and treatments (confocal microscopy).

A: LD - long-day reared, active variant, B: SDA - diapausing, cold-acclimated variant. LD Pro50 – LD larvae supplemented with 50 mg proline per g diet, SC: larvae supercooled to -5°C without freezing, F: larvae frozen at -5°C. Larvae were cooled gradually and held at target temperatures for 1 hour before rewarming (details in Figure S2). Tissues were dissected, fixed, and stained immediately after cold treatments. Larvae exposed to LN_2 were first pre-frozen to either -20°C or -30°C. Prewandering SDA larvae had recovered for approximately 3 weeks. Red: α-tubulin (anti-α-tubulin antibody), green: F-actin (phalloidin), blue: nuclei (DAPI). Biological replication (number of larvae) and technical replication (mean ± s.e.m. Malpighian tubules imaged per larva) are indicated below each image.

Table S1. Cold exposure regimes for malt fly larvae of various freeze tolerance states. LD: long-day (non-diapause, weakly freeze tolerant), LD Pro50: LD with dietary supplementation of 50 ± 5 mg proline per g of diet (non-diapause, moderately freeze tolerant), SDA: short-day acclimated (diapausing, extremely freeze tolerant), LN_2: liquid nitrogen, F: freeze treatment at -5°C (larvae in tubes were overlain with an ice crystal to ensure inoculation and freezing, verified by an exotherm), SC: supercooled (larvae cooled to -5ºC did not freeze as verified by a lack of exotherm). Recovered larvae were returned to rearing conditions at +18°C immediately after cold exposure and assessed after 3 days (LD), 1 week (SDA), or upon reaching the prewandering stage (SDA, approximately 3 weeks). Details of acclimations and cold exposure regimes are provided in Supplementary Material Figs. S1 and S2. Survival details from Rozsypal et al. (2018).

Treatment	Exposure temperature (°C)	Survival to adulthood (%)
LD +18	+18	91
LD -5 SC	-5 (unfrozen)	72*
LD -5 F	-5 (frozen)	39
LD -5 F (recovery, 3-day)	-5 (frozen)	39
LD -20	-20	0
LD Pro50 +18	+18	75
LD Pro50 -20	-20	34
SDA +4	+4	86
SDA -5 F	-5 (frozen)	76-86
SDA -20	-20	76-86
SDA -30	-30	76
SDA -30 (recovery, 1-week)	-30	76
SDA -30 (recovery, prewandering)	-30	76
SDA -20 LN_2	-196 (pre-frozen to -20°C)	0
SDA -30 LN_2	-196 (pre-frozen to -30°C)	39

*Determined in the present study